Research Square

Preprints are preliminary reports that have not undergone peer review.
They should not be considered conclusive, used to inform clinical practice,
or referenced by the media as validated information.

The Bacterial Gq Signal Transduction Inhibitor Fr900359 Impairs Soil-associated and Plant Pathogenic Nematodes

Wiebke Hanke
University of Bonn
Judith Alenfelder
University of Bonn
Jun Liu
Max Planck Institute for Neurobiology of Behavior – CAESAR
Philipp Gutbrod
Bonn International Graduate School – Land and Food, University of Bonn
Stefan Kehraus
University of Bonn
Max Crüsemann
University of Bonn
Peter Dörmann
University of Bonn
Evi Kostenis
University of Bonn
Monika Scholz
Max Planck Institute for Neurobiology of Behavior – CAESAR
Gabriele M. König (g.koenig@uni-bonn.de)
University of Bonn

Research Article

Keywords: FR900359, Chromobacterium vaccinii, soil microbiome, nematodes, Heterodera schachtii, Caenorhabditis elegans

Posted Date: May 25th, 2023

DOI: https://doi.org/10.21203/rs.3.rs-2965653/v1

License: This work is licensed under a Creative Commons Attribution 4.0 International License.
Read Full License

Abstract

The cyclic depsipeptide FR900359 (FR) is derived from the soil bacterium *Chromobacterium vaccinii* and known to bind G_q proteins of mammals and insects, thereby abolishing the signal transduction of their G_q protein-coupled receptors, a process that leads to severe physiological consequences. Due to their highly conserved structure, G_q family of proteins are a superior ecological target for FR producing organisms, resulting in a defense towards a broad range of harmful organisms. Here, we focus on the question whether bacteria like *C. vaccinii* are important factors in soil in that their secondary metabolites impair, e.g., plant harming organisms like nematodes. We prove that the G_q inhibitor FR is produced under soil-like conditions. Furthermore, FR inhibits heterologously expressed $G\alpha_q$ proteins of the nematodes *Caenorhabditis elegans* and *Heterodera schachtii* in the micromolar range. Additionally, *in vivo* experiments with *C. elegans* and the plant parasitic cyst nematode *H. schachtii* demonstrated that FR reduces locomotion of *C. elegans* and *H. schachtii*. Finally, egg-laying of *C. elegans* and hatching of juvenile stage 2 of *H. schachtii* from its cysts is inhibited by FR, suggesting that FR might reduce nematode dispersion and proliferation. This study supports the idea that *C. vaccinii* and its excreted metabolome in the soil might contribute to an ecological equilibrium, maintaining and establishing the successful growth of plants.

Introduction

Nematodes are ubiquitously distributed in soil (Bardgett and van der Putten, 2014; van den Hoogen et al., 2019) and present a widespread phylum with huge diversity (Porazinska et al., 2009; Song et al., 2017; Kouser et al., 2021; Lazarova et al., 2021). Their functional role in soil has been investigated intensively due to their impact on the soil food web and soil health (Ingham et al., 1985; Procter, 1990; Ferris, 2010; Lazarova et al., 2021; Melakeberhan et al., 2021). Nematodes are divided into trophic groups depending on their food source, i.e., bacterivore, fungivore, omnivore, herbivore, and predator (Yeates et al., 1993; van den Hoogen et al., 2019). Herbivorous nematodes, i.e., plant-parasitic nematodes, are known plant pathogens causing 12.3% of crop losses, equal to 157 billion US Dollar annually (Singh et al., 2015). The other trophic groups are known beneficial nematodes (Trap et al., 2016), e.g., predators like entomopathogenic nematodes (Koppenhöfer et al., 2020) are lethal for insect pests and utilized as biocontrol agents in agriculture (Dillman and Sternberg, 2012; Kenney and Eleftherianos, 2016). To sustain plant health, it is important to understand the equilibrium of beneficial and pathogenic effects present in soil, e.g., through investigations of interactions of soil organisms and their excreted metabolites.

The cyclodepsipeptide FR900359 (FR) (Fig. 1) is a member of a small family of natural products known as chromodepsins (Hermes et al., 2021a). The monomeric side chain of FR, *N*-propionylhydroxyleucine (*N*-Pp-OH-Leu), is attached via an ester bond to a hydroxyl group of one of the OH-Leu units of the macrocyclic part of the molecule. FR is produced by "*Candidatus* Burkholderia crenata", an endosymbiotic nonculturable bacterium with a highly reduced genome living in the leaf nodules of the

higher plant *Ardisia crenata* (Fujioka et al., 1988; Miyamae et al., 1989; Crüsemann et al., 2018). Biosynthesis of FR is performed by two nonribosomal peptide synthetase systems, encoded by the biosynthetic gene cluster (BGC) *frs* consisting of *frsA*-*H* (Crüsemann et al., 2018; Hermes et al., 2021b). After discovery of the *frs* BGC, database sequence searches allowed us to identify the cultivable and free-living soil bacterium *Chromobacterium vaccinii* as an additional FR producer (Hermes et al., 2021b). Other structurally related chromodepsins, i.e. FR-3 (sameuramide), were also found in an ascidian of the family *Didemnidae* (Yamashita et al., 2011), and another FR congener termed YM-254890 (YM) (Fig. 1) and its derivatives were reported from the soil bacterium *Chromobacterium* sp. QS3666, isolated in Japan (Taniguchi et al., 2003a). The structure of YM (Fig. 1) is almost identical to that of FR, differing only at two positions, (i) the side chain is composed of *N*-acetylhydroxyleucine (i.e. an acetyl instead of a propionyl moiety), and (ii) instead of the *N*-acetylhydroxyleucine unit in FR, YM possesses a *N*-acetylthreonine residue in the macrocyclic part (Fig. 1) (Taniguchi et al., 2003b).

FR and YM interact with $G\alpha_q$ proteins and thereby inhibit G_q-mediated nucleotide exchange with high selectivity at micromolar potency (Schrage et al., 2015). YM and FR differ in their residence time, but not in their binding affinity or inhibitory potency towards $G\alpha_q$ (Kuschak et al., 2019; Voss et al., 2021). This makes them both extremely useful tools to study G_q-mediated signaling of G protein-coupled receptors (GPCR) (Kamato et al., 2017; Kostenis et al., 2020). The latter are responsible for many major physiological processes and the target of approx. 35 % of our pharmaceutical drugs (Insel et al., 2019). Interestingly, there are only four major Gα protein families, $G\alpha_q$ being on of them (Downes and Gautam, 1999). G_q is hence part of many of the over 800 different GPCR-dependent signaling pathways. Thus, with chromodepsins like FR and YM, it is possible to modulate with a single active substance (e.g., FR or YM) the response of many GPCRs. This may be highly relevant for both the medical use and the ecological impact of FR and YM. Medically important findings include possible treatment of airway disorders (Carr et al., 2016; Matthey et al., 2017), reduction of adipositas (Klepac et al., 2016), and suppression of uveal melanoma (Annala et al., 2019; Lapadula et al., 2019; Onken et al., 2022), whereas the ecological effect of FR has mainly been researched towards insects (Crüsemann et al., 2018).

Indeed, as previous experiments towards insects and mammals showed, FR may function in nature as a protectant for the bacterial producer and, as in the case of endosymbiotic bacteria, its host plants. FR displays strong affinity towards Sf9 insect cell membranes and G_q proteins of the *Bombyx mori* and *Bemisia tabaci*. A second experiment using nymphs of the beetle *Riptortus pedestris* measured their survival rate after exposure to different FR concentrations over 9 days. For the two highest FR concentrations, 40 µM and 200 µM, the survival rate started to decline drastically after 4 days, with all insects being dead after seven days (Crüsemann et al., 2018). FR activity was also tested in mice (Matthey et al., 2017) and rats (Miyamae et al., 1989) to investigate its effects on mammals. Intratracheal application of FR in mice lead to airway relaxation, which may be of medical importance (Matthey et al., 2017), but systemic oral application in mice and rats resulted in decreased blood pressure and transient bradycardia (Miyamae et al., 1989; Matthey et al., 2017; Meleka et al., 2019).

Given its selective and potent activity, it can be assumed that the structures of FR and YM were evolutionary optimized for G_q inhibition. Structural changes in most positions of the backbone and side chain caused a drastic loss of activity (Xiong et al., 2016; Zhang et al., 2018; Xiong et al., 2019), e.g., FR-Core (Fig. 1), a FR molecule without the *N*-propionylhydroxyleucine side chain is 13-fold less active in dynamic mass redistribution (DMR) assays than FR and shows 207-fold lower binding affinity to its target than FR itself. It was thus hypothesized, that FR-Core is the evolutionary ancestor molecule of FR and, considering G_q inhibition as a trait for positive selection, that side chain biosynthesis evolved by duplications of sequences within *frs* (Hermes et al., 2021b).

The FR producing bacterium *C. vaccinii* MWU205 has originally been isolated from wild cranberry bog soil (Soby et al., 2013). If this bacterial strain indeed produces FR *in situ*, it could protect plants growing in bacteria-containing soil from pathogens like plant pathogenic nematodes. To date, *C. vaccinii* was only cultivated for FR production under laboratory conditions and it is not clear, whether chromodepsins like FR are produced in soil. We therefore started experiments to investigate whether *C. vaccinii* is able produce FR under soil-like conditions, and if FR is secreted by the producer bacterium into its surrounding. Next, we used our knowledge regarding the FR-binding site to approximate sensitivity of G_q proteins of nematodes to FR *in silico*, which was subsequently substantiated by *in vitro* assays using heterologously expressed nematode $G\alpha_q$. Most importantly, ecological relevant effects of FR on the soil-associated nematodes model organism *Caenorhabditis elegans* and *Heterodera schachtii*, a plant parasitic nematode, were observed *in vivo*. In these experiments FR affected locomotion and egg-laying of *C. elegans*. Similarly, experiments with *H. schachtii* resulted in inhibition of locomotion and hatching of juvenile stage 2 (J2) nematodes by FR.

Our data suggest that bacteria like *C. vaccinii* are important members of the soil microbiome, as their biosynthetic products may contribute to an ecological equilibrium and may even serve to protect plants from detrimental nematodes.

METHODS AND MATERIALS

General Experimental Procedures - Nuclear magnetic resonance (NMR) spectra were recorded on a Bruker Ascend 600 NMR spectrometer operating at 600 MHz (^{1}H) and 150 MHz (^{13}C) using $CDCl_3$ as solvent (Deutero GmbH; 99.8% D). NMR spectra were processed using Bruker Topspin Version 1.3 or MestReNova 8.0.1 software. Spectra were referenced to residual solvent signals with resonances at $\delta_H/_C$ 7.26/77.0. High-performance liquid chromatography mass spectrometry (HPLC/MS) data were recorded on a Waters 2695 separation module, which was coupled to a Waters 996 photodiode array detector, and a Waters QDa detector with electrospray ionization source. For separation a gradient elution with mobile phases A (acetonitrile/water 5/95 with 5 mM ammonium acetate and 40 µL acetic acid per Liter) and B (acetonitrile/water 95/5 with 5 mM ammonium acetate and 40 µL acetic acid per liter) on a Waters X Bridge Shield RP_{18} column (100 x 2.1 mm; 3.5 µm) at 25°C were used (flow of 0.3 mL/min, 80/20 A/B to 0/100 A/B within 20 min, and hold for 10 min). MS data were collected in positive and negative mode in

the range between *m/z* 140–1250 and additionally in the positive single ion mode for the mass trace of FR (*m/z* 1002.5; $M + H^+$). HPLC was carried out either using a Waters HPLC system, controlled by Waters Millenium software, consisting of a 600E pump, a 996 PDA detector, and a 717 plus autosampler or on a Waters Breeze HPLC system equipped with a 1525µ dual pump, a 2998 photodiode array detector, and a Rheodyne 7725i injection system.

Sample and Organism Collection - *C. vaccinii* MWU205 (DSM 25150, ATCC BAA 2314) was purchased from the German Collection of Microorganisms and Cell Cultures, DSMZ. *H. schachtii* was kindly provided by Dr Philipp Gutbrod. *C. elegans* strains N2, *egl-30(n686)*, *egl-30(ad806)*, *egl-30(ad805)*, *dgk-1(sy428)*, *eat-16(sa609)*, and *Escherichia coli* strain OP50 were provided by the Caenorhabditis Genetics Center, which is funded by NIH Office of Research Infrastructure Programs (P40 OD010440). *C. elegans* was maintained at 20°C using standard methods.

Topsoil was sampled in a garden on the 2nd of April 2019 (Dortmund Eichlinghofen, North Rhine-Westphalia: 51°28’35.0“N 7°24’22.1“E) and dried at room temperature for seven days on paper. Soil was sieved to remove rocks or plant debris and stored at 4°C.

Cultivation and Extraction of C. vaccinii - Lysogeny broth (LB) medium was prepared using 10 g/L NaCl, 10 g/L tryptone, 5 g/L yeast extract. A LB agar plate was inoculated with a cryoculture, cultivated for 2–4 days at 25°C, and used afterwards to inoculate 20 mL LB medium for preculture. The preculture was grown for 24 h at 25°C and 180 rpm. Subsequently the main culture (1.5 L LB medium) was cultivated with 1% of the preculture and 1‰ of carbenicillin (final concentration of 50 µg/mL) at 25°C and 160 rpm for 36–48 h. Extraction was performed with *n*-butanol (1:1) overnight, followed by centrifugation at 4,000 rpm for 10 min. The upper phase was collected and evaporated.

Isolation of FR and FR-Core - Each purification step was accompanied by MS analysis of the fractions. The crude material was fractionated on a Reveleris C_{18} flash column (220 g, 40 µm). A stepwise gradient solvent system of increasing polarity and a flow rate of 65 mL/min was used starting with 50/50 H_2O/MeOH for 13 min, then changing to 30/70 H_2O/MeOH within 1 min and hold again for 13 min. The gradient was changed then within 1 min to 25/75 H_2O/MeOH and hold for 25 min, then within 1 min to 20/80 H_2O/MeOH, hold for 13 min, then within 1 min to 15/85 H_2O/MeOH and hold for 25 min. Finally, the gradient was changed within 1 min to 100% MeOH and hold for additional 10 min. According to the measured evaporative light scattering detector (ELSD) and UV signals, a FR containing fraction was collected at 70 min. Final purification was done by HPLC with a semi-preparative Macherey-Nagel Nucleodur C_{18} column (250 x 8 mm, 5 µm) using an isocratic elution with 20/80 H_2O/MeOH (flow 2.0 mL/min). Pure FR was isolated as a white powder (FR: t_R: 20 min). The identity and purity were confirmed using NMR (Supplementary Figures S11-S12). FR-Core was isolated as described elsewhere (Hermes et al., 2021b).

FR Calibration Curve - Eight different concentrations of FR (purity > 90%) in HPLC/MS grade methanol (0, 0.0001, 0.0005, 0.001, 0.005, 0.01, 0.05, 0.1 mM FR) were prepared for HPLC/MS analyses. For small

concentrations, calibration curves were calculated using the four smallest concentrations. Visualization was performed using Prism 9.5.0.

Cultivation of C. vaccinii *in Soil-Extracted Medium* - Soil was extracted using the soil-extracted solubilized organic matter (SESOM) protocol (Vilain et al., 2006). Therefore 100 mg of soil were mixed with 0.5 L 3-(*N*-morpholino)propanesulfonic acid (MOPS) buffer (1.05 g MOPS, 0.09 g disodium EDTA, and 0.10 g sodium acetate were solved in water, and pH was adjusted to 7 at 40°C) and shaken at 160 rpm for two hours. Afterwards the whole mixture was filtered multiple times (folded filter paper for qualitative work, then vacuum filtration using 5 µm and subsequently 0.45 µm polyvinylidene fluoride filters). The pH of the extract was adjusted to 7.1–7.3 and the whole extract was subsequently sterile filtered (0.2 µm polyether sulfone membrane). For chitin experiments, chitin was autoclaved directly in the bottle used for sterile filtration of the final SESOM (final chitin concentration: 1 g/L) now called SESOM (+). Both SESOM and SESOM (+) were tested for sterility by inoculation of a LB plate and incubating it at 37°C for 24 h.

Precultures for SESOM experiments were grown in LB medium inoculated with *C. vaccinii* grown on LB plates for 2–4 days at 25°C. The preculture was supplemented with carbenicillin disodium salt to a final concentration of 50 *µ*g/mL. After cultivation at 25°C for 24 h the preculture was centrifuged at 5.000 rpm for 5 minutes. The pellet was washed two times with 0.9% NaCl solution. Afterwards the colony-forming units (CFU) were determined by plate count and inoculation was performed with $3.2*10^4$ CFU/µL for SESOM and $5.2*10^6$ CFU/µL for SESOM (+). For SESOM 2x80 mL were inoculated. One culture was separated at the start (0 days) into three samples à 25 mL, which were directly extracted. The second culture was separated similar after 5 days of cultivation at 25°C and 180 rpm. One blank was prepared using only SESOM. Extraction (1:1) was performed for 6 h at 180 rpm using *n*-butanol. Afterwards the whole extract was centrifuged for 15 min at 4,000 rpm and the upper phase was evaporated. For analysis via HPLC/MS 1 mg/mL solutions were prepared using HPLC/MS grade methanol. For SESOM (+), eight 50 mL flasks containing 30 mg chitin were sterilized and afterwards filled with SESOM. One flask was not inoculated and directly extracted as blank. Seven flasks were inoculated and three of these flasks were extracted (0 days). Four flasks were cultivated at 25°C and 180 rpm and extracted after five days. Extraction (1:1) was performed over night at 180 rpm using *n*-butanol. Subsequently the whole extract was centrifuged for 15 min at 4,000 rpm and the upper phase was evaporated. For analysis via HPLC/MS, 2 mg/mL solutions were prepared using HPLC/MS grade methanol.

FR Secretion Experiment – The preculture was made as described in "*Cultivation and Extraction of C. vaccinii*". Main cultures (6 times) were prepared using 25 mL LB medium inoculated with the preculture (1%). The preculture and main cultures were supplemented with carbenicillin disodium salt to a final concentration of 50 *µ*g/mL. After 43 h the main culture was centrifuged at 5,000 rpm for 5 min, the pellet was washed two times with 2.5 mL 0.9% NaCl-solution and centrifuged again. All three supernatants were combined and extracted with 30 mL *n*-butanol. Additionally, the pellet was extracted with *n*-butanol, sonicated shortly, and shaken over night at 180 rpm. After centrifugation at 4,000 rpm for 10 min, the *n*-butanol phase was evaporated. All extracts (supernatant and pellet) were weight and solved for HPLC/MS with HPLC/MS grade methanol to a concentration of 2 mg/mL.

Bioinformatical Alignment and Visualization - The Basic Local Alignment Search Tool (BLAST) (Altschul et al., 1997; Altschul et al., 2005) was utilized using the amino acid sequence of the $G\alpha_q$ isoform a of *C. elegans* (UniProt: G5EGU1) as query. Standard databases (non-redundant protein sequences) were selected as search set but restricted to the organisms belonging to Nematoda. The blastp algorithm was used with default parameters.

Sequences were aligned using the Clustal W alignment tool in MEGA 11 (Version 11.0.11). For the pairwise alignment, a penalty of 10 for gap opening and 0.1 for gap extension were selected. For the multiple alignment, the penalty for gap opening was the same, but gap extension was punished with 0.2. Gonnet was chosen as protein weight matrix, and residue-specific and hydrophilic penalties were switched on. Concerning gap separation, a matrix of four and no end were selected. No negative matrix was used, and the delay divergent cutoff was set at 30%.

Depictions of YM in complex with a chimeric $G_{i1/q}$ protein were created with PyMOL™ 2.5.4 (Schrodinger) from PDB ID 3AH8 (Nishimura et al., 2010).

Cell Culture and Transient Transfection - Cell culture materials were purchased from Invitrogen. The $G\alpha_{q/11}$ knock-out HEK293 cells (HEK-$\Delta G_{q/11}$) were generated by CRISPR-Cas9 technology as described previously in detail (Schrage et al., 2015). Cells were cultivated in Dulbecco's modified Eagle's medium, supplemented with 10 % (v/v) fetal calf seum, penicillin (100 U/mL) and streptomycin (0.1 mg/mL), at 5 % CO_2 and 37°C in a umidified atmosphere. All monthly tests for mycoplasma contamination by PCR were negative.

HEK-$\Delta G_{q/11}$ cells were transfected in suspension 48 h prior to the experiments using polyethylenimine (1 mg/mL, Polyscience) following the manufacturer's protocol. A total amount of 8 µg plasmid (3 µg, 0.6 µg, 2 µg of expression plasmids containing HA-tagged $G\alpha_q$ isoforms, muscarinic acetylcholine M3 receptor, and RIC-8A, respectively, filled up with pcDNA3.1(+)) and 24 µL PEI solution were added to 2.8 x 106 cells plated in 10 cm dishes.

IP_1 Accumulation Assay - The IP_1 accumulation was measured using homogeneous time resolved fluorescence (HTRF) technology (Cisbio) following the manufacturer's instructions. For this, transfected HEK-$\Delta G_{q/11}$ cells were detached and washed in PBS. After resuspension in LiCl-containing assay buffer stopping breakdown of IP_1, cells were seeded into white 384-well plates with 50,000 cells per well. Carbachol and FR were added simultaneously, followed by 40 minutes of incubation at 37°C. Subsequently, cells were lysed and incubated with d2-labeled and cryptate-labeled IP_1 antibodies for a minimum of 60 minutes at room temperature. The HTRF ratio values measured with a Mithras LB 940 multimode plate reader (Berthold Technologies) were converted to IP_1 concentrations in nM using an IP_1 (unlabeled) standard curve.

Calcium $^{2+}$ Mobilization Measurement - Calcium^{2+} mobilization was measured using FLIPR Calcium 5 assay kit using the Flex Station 3 MultiMode Benchtop reader (both Molecular Devices), as described

elsewhere (Patt et al., 2021) with slight modifications. Briefly, 24 h after transfection, HEK-$\Delta G_{q/11}$ cells transferred to flat-bottom 96-well cell culture plates at a density of 60,000 cells per well. On the day of the assay, cells were incubated in Calcium 5 dye for 45 min at 37°C before 1 to 3 dilutions with Hanks' Balanced Salt Solution + 20 mM HEPES. For preincubation with inhibitor, FR was added to the dye in the appropriate concentrations. Kinetic fluorescence measurements (baseline read and addition of agonist or buffer after 20 s) were performed to assess calcium^{2+} release from intracellular stores.

Western Blotting - HEK-$\Delta G_{q/11}$ cells were washed and lysed on ice with a mix of lysis buffer (25 mM Tris, pH 7.4, 150 mM NaCl, 1 mM EDTA, 1% Triton X-100, 1% IGEPAL) and protease inhibitor mixture (Sigma). After 20 min of shaking, lysates were spun down (16,100 x g, 10 min). Protein levels in the supernatant were determined with the Pierce BCA Protein Assay (Thermo Fisher Scientific). Protein separation was achieved by SDS-polyacrylamide gel electrophoresis (SDS-PAGE) and electroblotted onto a nitrocellulose membrane (Hybond-C Extra, GE Healthcare). Membranes were blocked with Roti-Block (Carl Roth) and successively incubated with primary mouse anti-hemagglutinin (HA) (1:1,000) and secondary Horseradish Peroxidase (HRP)-conjugated goat anti-mouse antibody (1:10,000). For detection, the Amersham Biosciences ECL Prime Western blotting detection reagent (GE Healthcare) was added. Membranes were subsequently washed and reprobed with rabbit anti-α-tubulin (1:1,000) and HRP-conjugated goat anti-rabbit antibody (1:10,000) to control for equal loading. Membrane bands were quantified with ImageJ (Schneider et al., 2012).

C. elegans *Synchronization* - The investigated pathway directly impacts developmental timings of the worm. To compare animals at the same age, we measured the developmental time from egg to adulthood for all strains. We found that mutant worms at 20°C needed 6 h more to reach adulthood than wildtype. For the locomotion experiments, the animal culture times were offset to allow delayed mutants to develop until the correct age. As checks for egg-laying during the locomotion experiments revealed the suppressor mutants, *dgk-1*(*sy428*), and *eat-16*(*sa609*), to be slower their delay was lengthened to 10 h for the subsequent egg-laying experiments. Synchronization of *C. elegans* wildtype N2, *egl-30*(*ad806*), *egl-30*(*ad805*), *egl-30*(*n686*), *dgk-1*(*sy428*), and *eat-16*(*sa609*) was performed using bleaching solution (2 mL 5% sodium hypochlorite, 1.5 mL 5M potassium hydroxide, and 6.5 mL ddH_2O), M9 buffer and *C. elegans* grown for 3–4 days on a 10 cm NGM plate at 20°C. Nematodes were washed off with M9. After centrifugation and removal of 900 µL, 1 mL of bleaching solution was added to the pellet. The sample was mixed for 2 minutes and centrifuged afterwards. This step was repeated a second time. Afterwards the pellet was washed three times with M9 to remove the bleach solution and resuspended in 1 mL of M9 buffer. Finally, eggs were counted, and concentration was adjusted to a maximum of 5 eggs/µL, if necessary, and rotated overnight to synchronize to larval stage 1 (L1).

C. elegans *Tracking Experiment* - Approximately 100 synchronized *C. elegans* N2, *egl-30*(*ad805*), *egl-30*(*n686*), *egl-30*(*ad806*), *dgk-1*(*sy428*), *eat-16*(*sa609*) L1 were grown on NGM with a spot (40 µL) *E. coli* OP50 mixed with FR (2.5 mM) in 1% DMSO or just 1% DMSO as control. After approx. 55 h (N2) plus above-mentioned offset for mutant worms were imaged. Imaging of worms was performed using a commercial upright epifluorescence microscope (Axio Zoom V16; Zeiss) equipped with a 1x objective

(PlanNeoFluar Z 1.0x/N.A. 0.25). Brightfield image was performed and imaged on camera (BASLER; acA3088-57um) using a camera adapter with an additional 0.5x magnification (60N-C ″ 0.5x; Zeiss) resulting into an effective magnification on camera of 0.35x. Animals were imaged at 15 fps for 5 min unless otherwise indicated.

Animals were tracked using the tracking package trackpy (Allan et al., 2019) with a custom detection script in Python based on the pharaglow package (Bonnard et al., 2022). The animal speed was calculated from the resulting center-of-mass coordinates as follows: The trajectories (x, y, t) were sub-sampled from 14 fps to 2.8 fps and the speed was calculated as $v\left(t_2\right)=\sqrt{\frac{\left(x_{t2}-x_{t1}\right)^2+\left(y_{t2}-y_{t1}\right)^2}{dt}}$ with $dt=\frac{1}{2.8}s$.

The animals' spatial distribution was evaluated by counting nematodes inside the lawn and outside the lawn, where outside the lawn meant that no part of the worm touched the lawn. Border crossings were counted in a similar way as the recorded tracks were evaluated and each crossing independent of the direction (leaving or entering) was counted.

C. elegans *Egg-Laying Experiment* - Approx. 50 synchronized *C. elegans* N2, *egl-30*(*ad806*), *egl-30*(*n686*), *dgk-1*(*sy428*), *eat-16*(*sa609*) L1 were grown on NGM plates completely covered with *E. coli* OP50 mixed with FR (2.5 mg/mL) in 1% DMSO or 1% DMSO as control for 72 h (N2), 78 h (*egl-30*(*n686*), *egl-30*(*ad806*)), and 81 hours (*dgk-1*(*sy428*), *eat-16*(*sa609*)). Afterwards 12 worms per genotype were picked and put separately on plates completely covered with the mixtures described before. After two hours the nematode was removed from the plate and eggs were counted.

C. elegans *Retained Eggs Experiment* - Approx. 100 synchronized *C. elegans* N2, *dgk-1*(*sy428*), *eat-16*(*sa609*) L1 were grown on NGM plates completely covered as described for the egg-laying experiment. After 72 h (N2) and 81 h (mutants), 20 worms were picked and put separately in 10 µL drops of 6% bleaching solution (5% sodium hypochlorite solution solved in dH_2O) for 15 min.

H. schachtii *Cultivation* - *H. schachtii* was cocultivated with *Sinapis alba* to generate cysts and J2 used for the activity and cyst assay (Sijmons et al., 1991).
H. schachtii *Activity Assay* - Approximately 100 J2 were added to 500 µL volume containing 1% DMSO mixed with or without 1 mM FR. Additionally one experiment was conducted by adding 50 µL octopamine to control and FR. After 4 d the number of active J2 were counted. For the concentration-dependency experiment different concentration of FR (0.0624 mM, 0.125 mM, 0.25 mM, 0.5 mM) were added and counted after 4 d (Gutbrod et al., 2020).
H. schachtii *Cyst Assay* - Approximately 20 cysts were added to 500 µL volume containing 1% DMSO mixed with or without 0.01 mg/mL FR. Each experiment was replicated 4 times and cultivated for 7 d at room temperature. Afterwards the number of J2 was counted per experiment and divided by the number of cysts in the well.

Statistical Analyses - Data and statistical analyses were performed using GraphPad Prism version 9.5.0 as described in detail below. To evaluate the spatial distribution of *C. elegans* a *modified two sample binomial test* (Wong et al., 2014) was performed using Microsoft Excel. Raw data for all statistical tests performed is summarized in Online Resource 2.

SESOM, SESOM with chitin, and the secretion experiment were tested for normality using the *Shapiro-Wilk test*, which stated them to be normally distributed. Afterwards the *unpaired t-test* for both SESOM experiments and the *paired t-test* for the secretion experiment were utilized. Summarized data represent the data of three technical replicates for SESOM, three or four replicated for SESOM with chitin, and six replicates for the secretion experiment. For the FR calibration curve for SESOM the fours smallest concentrations were picked and for the secretion experiment all eight concentrations were chosen and used to calculate a simple linear regression using Prism 9.5.0.

C. elegans experiments concerning velocity, egg-laying rate, and retained eggs were tested for normality or lognormality using *D'Agostino & Pearson test*. For velocity all three *egl-30* mutants, *egl-30*(*ad805*), *egl-30*(*n686*), and *egl-30*(*ad806*) were found to have a log-normal distribution while N2, *dgk-1*(*sy428*), and *eat-16*(*sa609*) were not normally distributed. Subsequently, the *Mann-Whitney test* was performed for N2, *dgk-1*(*sy428*), and *eat-16*(*sa609*) and the *unpaired t-test* was performed for all three *egl-30* mutants to compare control against FR. For the egg-laying rate, all five genotypes (N2, *egl-30*(*n686*), *egl-30*(*ad806*), *dgk-1*(*sy428*), and *eat-16*(*sa609*)) were found to be normally distributed. Subsequently the *unpaired t-test* was chosen for the comparison of Control versus FR. For the retained eggs assay, *C. elegans* N2 and *eat-16*(*sa609*) displayed normally distributed data, while *dgk-1*(*sy428*) was not normally distributed. Accordingly, *unpaired t-tests* were performed to compare Control vs. FR for *C. elegans* N2 and *eat-16*(*sa609*), while the *Mann-Whitney test* was used for *dgk-1*(*sy428*).

Regarding *H. schachtii*, experiments evaluating the effect of FR and octopamine on the activity of nematodes, *One-Way-ANOVA* with *Tukey's multiple comparisons test* was performed as data passed the *Shapiro-Wilk test* for normality. To investigate the effect of FR on hatching of J2 *H. schachtii*, the *unpaired t-test* was performed as data passed the *Shapiro-Wilk test* for normality. Summarized data represent the data of four technical replicates.

RESULTS

Production and excretion of FR by C. vaccinii *MWU205 under soil-like conditions.* The functional assessment of single members of a microbiome is extremely difficult. Apart from the fact that only a small percentage of soil bacteria can be cultivated in the laboratory (van Pham and Kim, 2012; Fierer, 2017), their interactions and their secondary metabolite production under natural conditions are mostly unknown (Berendsen et al., 2013). Additionally, the *in situ* relevance of natural products is often not clear. To date we failed in cultivating *C. vaccinii* in the laboratory in soil directly. Even though this bacterium was shown to produce FR and derivatives under standard laboratory conditions (Hermes et al., 2021b), it

is not clear whether secondary metabolite production also occurs under natural or close to natural conditions.

To address whether FR is produced and secreted by *C. vaccinii* under soil-like conditions, we decided to use soil extracts, particularly soil-extracted solubilized organic matter (SESOM), as a liquid medium. SESOM applies 3-(*N*-morpholino)propanesulfonic acid (MOPS) buffer for soil extraction. The resulting extract can be used for bacterial cultivations (Vilain et al., 2006). We collected soil samples, extracted SESOM, and applied it to cultivate *C. vaccinii* for 5 days at 25°C. In a second experiment we added the natural polymer chitin to SESOM to supplement a potential carbon and nitrogen source from soil, as genes encoding for chitinases have been reported in the genome of *C. vaccinii*, (Vöing et al., 2015). Extraction with *n*-butanol was done after inoculation (0 days) and after 5 days of cultivation, followed by analysis of the extracts via HPLC/MS, calculation of FR concentrations via calibration curves (Supplementary Fig. S1 of Online Resource 1), and comparison of the FR concentrations of the different experiments. Both experiments (i.e., with and without chitin) presented a significantly increased FR concentration after five days of cultivation, 15-fold for SESOM (*two-tailed unpaired t-test*: $p = 0.0005$) (Fig. 2a) and 2-fold (*two-tailed unpaired t-test*: $p = 0.0121$) for SESOM with chitin (Supplementary Fig. S2 of Online Resource 1) compared to cultures immediately extracted after inoculation.

We also examined whether *C. vaccinii* not only produces, but also excretes FR. For this, we investigated the FR content in both, the pellet and the supernatant of *C. vaccinii* grown in LB medium. The supernatant contained a significantly (*paired t-test*: $p < 0.0001$) higher FR concentration as compared to the pellet (Fig. 2b). It is thus concluded, that under soil-like conditions the FR concentration is between 0.00010 mg/mL (SESOM alone) and 0.00007 mg/mL (SESOM plus chitin). Furthermore, FR is excreted by *C. vaccinii*, suggesting the presence of FR in soil inhabited by *C. vaccinii*.

Nematode G_q proteins and their FR-binding site. Nematodes are ubiquitously distributed in soil (Bardgett and van der Putten, 2014; van den Hoogen et al., 2019) and many of them feed on bacteria. Therefore, it is conceivable that FR is produced as a defense *inter alia* against nematodes by soil bacteria, such as those belonging to the genus *Chromobacterium* (Taniguchi et al., 2003a; Hermes et al., 2021b). Nematodes are also dreaded plant pathogens, which may be similarly affected by FR. This is quite plausible, since G_q proteins are highly conserved in most eucaryotes (Mendoza et al., 2014; Lokits et al., 2018).

To date, no data are available to judge the FR sensitivity of nematode G_q proteins. Hence, we searched for available G_q protein sequences from nematodes and aligned the respective putative FR-binding sites. Such *in silico* evaluations were thought to be very insightful, since the binding site of the FR related YM to the human G_q protein is known in detail and in parts confirmed for FR via mutagenesis and binding studies (Malfacini et al., 2019; Voss et al., 2021).

The bacteria-feeding nematode *Caenorhabditis elegans* is a well-studied model organism (Brenner, 1974; Harris et al., 2020; Davis et al., 2022). It expresses a $G\alpha_q$ ortholog with 82% amino acid sequence identity

to the murine $G\alpha_q$, as deduced from cDNA sequences. *C. elegans* $G\alpha_q$ is encoded by *egl-30*, and the respective protein plays a crucial role in nematode physiology, e.g., egg-laying, locomotion, pharyngeal activity, and axon regeneration (Brundage et al., 1996). To find further nematode $G\alpha_q$ sequences, we conducted a search with the Basic Local Alignment Search Tool (BLAST) (Altschul et al., 1997; Altschul et al., 2005) using the amino acid sequence of the $G\alpha_q$ isoform a of *C. elegans* (UniProt: G5EGU1), and restricting the organism group to the taxon Nematoda. The output (100 sequences) represented mostly sequences of parasitic nematodes known to infect humans and mammals with no direct connection to soil, and was consequently filtered, selecting only nematodes belonging to the genus *Caenorhabditis* (9 sequences) or being associated with soil (8 sequences). Additionally, the genome and transcriptome of *H. schachtii* were sequenced (Siddique et al., 2022) and subsequently searched by for probable $G\alpha_q$ orthologs. This way an mRNA consisting of 353 amino acids was identified and used for the alignment (Access to the sequences was provided to us by Dr Sebastian-Eves-van den Akker). A summary of all organisms used for the alignment can be found in supplementary tab. S1 of Online Resource 1.

G_q proteins are highly conserved in metazoa and essential for their life (Mendoza et al., 2014; Lokits et al., 2018). $G\alpha_q$, $G\alpha_{11}$, $G\alpha_{14}$, and $G\alpha_{16}$ belong to the $G\alpha_q$ family and FR potently inhibits all of them, except $G\alpha_{16}$. The putative FR-binding site has been investigated using the crystal structure of the FR-related depsipeptide YM (Fig. 1) with G_q (Fig. 3a) (Nishimura et al., 2010) and further mutagenesis and binding studies (Malfacini et al., 2019; Voss et al., 2021). Taken together, these studies show that FR binds to human G_q in the interdomain cleft between the helical (H) and GTPase domain (G) by interacting with linker I and switch I (linker 2) (Voss et al., 2021). It has been revealed that hydrophobic interactions are important for FR-binding, including positions in the human $G\alpha_q$ according to CGN nomenclature (Flock et al., 2015), $V182^{G.hfs2.1}$ and $V184^{G.hfs2.3}$, $I190^{G.S2.2}$, $E191^{G.S2.3}$, and $P193^{G.S2.5}$, followed by, $G74^{H.HA.6}$, $F75^{H.HA.7}$, and $L78^{H.HA.10}$. Furthermore, the polar aspartate $D71^{H.HA.3}$is crucial for a salt bridge formation with $R60^{H.H1.9}$, which stabilizes FR-binding via hydrogen bonds (Nishimura et al., 2010; Malfacini et al., 2019; Voss et al., 2021). Apart from these amino acid residues. eight others were predicted to directly or indirectly interact with YM and therefore, may also be relevant for FR-binding (Nishimura et al., 2010).

In our alignment, we compared 42 amino acid residues of the putative FR-binding region of the human $G\alpha_q$ protein with the corresponding sequences in nematode $G\alpha_q$ proteins to identify similarities and differences (Fig. 3b). To estimate the importance of any difference in the sequences of the FR-binding sites, the inhibitor binding was visualized in the YM-$G_{q/i}$ crystal structure (PDB code: 3AH8) using PyMOL™ 2.5.4 (Fig. 4) (Nishimura et al., 2010).

Within the 42 amino acid residues of the putative FR- and YM-binding site (Fig. 3), we identified seven positions which differ between the $G\alpha_q$ of nematodes as compared to the FR-sensitive human $G\alpha_q$ protein: position G.h1ha.2, G.h1ha.5, H.HA.1–2, and H.HA.6–8 (Fig. 3b). As shown in Fig. 4a the $S65^{G.h1ha.2}$ residue is distant to the inhibitor (> 6.9 Å), and a change at this position will most likely not affect FR- and YM-binding as previous studies suggest. In a similar way the changes at positions

S68$^{G.h1ha.5}$, D69$^{H.HA.1}$, E70$^{H.HA.2}$, and T76$^{H.HA.8}$ as depicted in Fig. 4a, are unlikely to influence FR- or YM-binding markedly, as the respective residues point away from the inhibitor, which is in line with studies already published (Nishimura et al., 2010).

A more profound influence on FR- and YM-binding might arise from changes in positions G74$^{H.HA.6}$ and F75$^{H.HA.7}$. While there is a glycine residue at H.HA.6 in the human $G\alpha_q$ protein, most nematode $G\alpha_q$ proteins contain an alanine or glutamine residue at this position, which represents a considerable change. Figure 4b illustrates that the distance between glycine in the heterotrimeric human $G_{i/q}$ chimeric protein and YM is 3.8 Å and changes at this position might influence FR- and YM-binding. Former experiments substantiate this assumption, as exchanging glycine to valine at this position leads to a faster dissociation of an FR-based radioligand [^{3}H]PSB-15900-FR (Voss et al., 2021).

F75$^{H.HA.7}$ is predicted by Nishimura et al. to directly interact with the FR congener YM (Nishimura et al., 2010), which is further supported for FR itself (Voss et al., 2021). F75$^{H.HA.7}$ is part of a hydrophobic network important to stabilize FR- and YM-binding and has approximately 4.1 Å distance to YM as predicted from the crystal structure (Fig. 4c). Our alignment revealed that 15 out of 17 sequences of nematodes contain histidine at H.HA.7, and all 17 $G\alpha_q$ sequences of nematodes (Fig. 3b) contain amino acids with aromatic residues, e.g., tyrosine, histidine or phenylalanine. As neither of these amino acids disrupts the hydrophobic network, this change is not considered to severely impact FR-binding.

Regions G.hfs2 and G.s2 (Fig. 3) of all $G\alpha_q$ proteins are clearly involved in YM- and FR-binding (Nishimura et al., 2010; Malfacini et al., 2019; Voss et al., 2021) and are identical between the $G\alpha_q$ proteins of all selected nematodes and the human ortholog.

Taken together, the $G\alpha_q$ proteins of nematodes are likely to be inhibited by FR and YM. There are two positions in $G\alpha_q$ proteins of nematodes which differ from human $G\alpha_q$ and possibly influence the binding of FR. To substantiate this further, we used *in vitro* investigations with $G\alpha_q$ of the nematode model organism *C. elegans* and the plant-parasitic *H. schachtii*.

Comparing both organisms used for the *in vitro* $G\alpha_q$ inhibition assay with FR, i.e., *H. schachtii* and *C. elegans*, a pairwise alignment of both full length $G\alpha_q$ amino acid sequences revealed 90% identity. Looking at the investigated FR-binding region of these two nematodes (Fig. 3) only three positions differ, G.h1ha.2, H.HA.1, and H.HA.6. As pointed out above the first two positions, G.h1ha.2 and H.HA.1, are supposedly not required for the interaction with the inhibitor (Fig. 4a), and only the difference at position H.HA.6 is seemingly of interest. Plant parasitic nematodes like *H. schachtii* have a more spacious residue with glutamine at position H.HA.6 compared to the alanine present in nematodes belonging to the *Caenorhabditis* group. As it is difficult to predict the influence of these changes on the binding and activity of FR, we investigated the inhibition of FR on nematode $G\alpha_q$ *in vitro*.

FR inhibits heterologously expressed Gα $_q$ proteins of C. elegans *and* H. schachtii in vitro. To verify our bioinformatic predictions we chose *H. schachtii* as representative for the plant pathogenic nematodes and *C. elegans* as representative for the bacteria-feeding nematodes and well-characterized model organism to investigate the sensitivity of these two nematode $G\alpha_q$ isoforms to FR *in vitro*.

The $G\alpha_q$ protein of *H. schachtii* was transiently introduced into HEK293 cells genetically edited with CRISPR/Cas9 technology to lack endogenous G_q and G_{11} proteins (HEK $G_{q/11}$-KO cells) to avoid signal confounding. As functional G_q readout, we measured the accumulation of inositol monophosphate (IP_1) after stimulation of the endogenously expressed muscarinic acetylcholine receptor type 3 (M3) with carbachol. However, even at concentrations as high as 100 µM carbachol, expression of *H. schachtii* $G\alpha_q$ did not increase the level of IP_1 over vector control, whereas expressing murine G_q resulted in increased IP_1 accumulation under the same conditions.

The lack of signal might be due to various reasons, ranging from improper protein folding or location to the missing of further proteins necessary for *H. schachtii* G_q signaling. One of these proteins might be resistant to inhibitors of cholinesterase 8A (RIC-8A), which was first identified as a crucial part of G_q signaling in the nematode *C. elegans* (Miller et al., 2000). Later, RIC-8 was shown to facilitate G protein folding and thereby expression (Chan et al., 2013) and to act as guanine-nucleotide exchange factor (GEF) (Tall et al., 2003). Moreover, it has previously been used to amplify signaling of other insect G proteins (Himmelreich et al., 2017). Based on this, we decided to co-express RIC-8A with *H. schachtii* $G\alpha_q$ to increase expression and enable signaling. However, RIC-8A co-expression alone did not result in a measurable response of the $G\alpha_q$ protein to carbachol. In a further attempt, we over-expressed the M3 receptor for G protein activation, which again, on its own, did not lead to an increase in IP_1 accumulation over vector control (Supplementary Fig. S3). Only the combination of both, RIC-8A and M3 expression, led to a concentration-dependent IP_1 accumulation upon carbachol addition as shown in Fig. 5a.

To investigate the FR sensitivity of *H. schachtii* $G\alpha_q$, we pre-incubated cells with varying concentrations of the inhibitor and stimulated with 10 µM carbachol as this concentration elicits the highest response. In line with our predictions from the alignment, FR was able to completely blunt *H. schachtii* G_q signaling with low micromolar potency (Fig. 5b).

To investigate the $G\alpha_q$ protein of *C. elegans*, we repeated the activation and inhibition experiments with HEK $G_{q/11}$-KO cells transiently expressing *C. elegans* $G\alpha_q$ cDNA. As is evident from Fig. 5c, *egl-30* can be functionally expressed in HEK $G_{q/11}$-KO cells when following the established protocol of over-expressing M3 and RIC-8A. Moreover, the activation behavior of *C. elegans* $G\alpha_q$ closely resembles that of *H. schachtii* $G\alpha_q$, considering that the shapes of the dose response curves are similar and the pEC_{50} values are comparable. Regarding inhibition, *C. elegans* $G\alpha_q$ is clearly FR-sensitive with full inhibition at 100 µM inhibitor and an IC_{50} value in the low micromolar range (Fig. 5d).

C. elegans is a well-known nematode model organism with a plethora of established experimental methods available, which allows studying FR effects more easily in this organism. Therefore, we were inclined to corroborate our findings with an additional read-out for the assessment of *C. elegans* $G\alpha_q$ activity. We chose to repeat the same set of activation and inhibition experiments now measuring the increase of intracellular calcium concentrations as consequence of G_q activation. Again, functional expression was achieved (Fig. 5e). Remarkably, when inhibiting with FR (Fig. 5f), the resulting dose-response curve was shifted to the left to a high nanomolar potency, showing a more moderate steepness of the curve compared with the IP_1 accumulation assay. These results confirm the ability of FR to inhibit *C. elegans* $G\alpha_q$.

Taken together, we were able to express functionally active $G\alpha_q$ proteins of *H. schachtii* and *C. elegans* in cell cultures and confirmed their inhibition by FR. Interestingly both, *H. schachtii* and *C. elegans* $G\alpha_q$, were inhibited with a similar potency in the IP_1 assay, implicating that the difference in the FR-binding site between both proteins, alanine as opposed to glutamine at position H.HA.6 is not interfering with FR activity, conceivable because a glutamine at this position might face away from the inhibitor. These promising *in vitro* results made *in vivo* effects very likely, which were thus the focus of our next experiments.

FR impairs movement, allocation, and egg-laying of C. elegans in vivo. To investigate the effect of FR on $G\alpha_q$ of *C. elegans*, we used *C. elegans* wildtype N2 and a set of three strains with different *egl-30* mutations to illustrate G_q loss-of-function phenotypes. The strong *egl-30*(*ad805*) mutant exhibits a severe egg-laying phenotype as it is nearly paralyzed and bloated with eggs, subsequently called “strong mutant”. Two hypomorphic mutants, *egl-30*(*n686*) and *egl-30*(*ad806*), are less bloated with eggs and sluggish to very sluggish, but never paralyzed, and termed “weak mutants” in this study (Brundage et al., 1996). Additionally, the G_q signaling suppressor mutants *dgk-1*(*sy428*) and *eat-16*(*sa609*) were utilized as opposing phenotypes. The suppressor mutant *dgk-1*(*sy428*) encodes a loss-of-function diacylglycerol kinase (DGK-1) (Jose and Koelle, 2005). DGK-1 is known to act as a negative regulator of G_q signaling, as it phosphorylates the second messenger diacylglycerol (DAG) (Miller et al., 1999). The suppressor mutant *eat-16*(*sa609*) is a missense loss-of-function mutant of *eat-16*. The latter encodes a negative regulator of G protein signaling, which belongs to the family of GTPase activating proteins (GAPs). It leads to hydrolysis of GTP and this way turns G proteins into their inactive state (Hajdu-Cronin et al., 1999). Both suppressor mutants display hyperactivity with fast movements and rapid egg-laying (Hajdu-Cronin et al., 1999).

$G\alpha_q$ is important for the locomotion of *C. elegans* (Brundage et al., 1996). Therefore, tracking experiments on agar plates were performed with nematodes raised as explained in the experimental section. Three repeats were performed for each of the six genotypes (*C. elegans* N2, *egl-30*(*ad805*), *egl-30*(*n686*), *egl-30*(*ad806*), *dgk-1*(*sy428*), *eat-16*(*sa609*)) and summarized in Fig. 6. Single tracking results can be found in supplementary fig. S4-S9 of Online Resource 1. The experimental set up included a spot of *Escherichia coli* OP50 bacteria in the middle of the agar plate (bacterial lawn on which the nematodes feed) and

allowed to analyze the velocity of nematodes and the spatial distribution of nematodes outside or in the bacterial lawn.

The velocity (Fig. 6a) of the controls (i.e., without FR treatment) of each genotype showed that both suppressor mutants, i.e., *dgk-1*(*sy428*) and *eat-16*(*sa609*), were the fastest moving genotypes, followed by the wildtype N2. Compared to that, all *egl-30* mutants, i.e., *egl-30*(*n686*), *egl-30*(*ad806*), and *egl-30*(*ad805*), were slower in movement. These results were consistent with the results from previous reports (Brundage et al., 1996; Hajdu-Cronin et al., 1999).

For the wildtype N2, FR reduced the average velocity significantly (*Multiple Mann-Whitney tests*: $p = 0.0076$) (Fig. 6a). The spatial distribution of *C. elegans* N2 was also affected by FR (Fig. 6b) as significantly less nematodes were inside the lawn, i.e., 92.2% without FR compared to 83.8% with FR (*Modified two sample binomial test* (*MBT*): $p = 0.0021$). All these results agree with the expected outcome of G_q inhibition.

FR did not affect the mean velocity (*Unpaired t-test*: $p = 0.9876$) of the strong mutant *egl-30*(*ad805*) or its spatial distribution (*MBT*: $p = 0.6818$) (Fig. 6). In this case, the data from one repeat were excluded from the analysis of the spatial distribution as the bacterial lawn of this repeat was enlarged unevenly (Supplementary Fig. S6b of Online Resource 1). Due to the already strongly impaired G_q signaling in this mutant strain, further G_q inhibition was not envisioned to have a major impact. These results are thus as expected.

For both weak *egl-30* mutants, *egl-30*(*n686*) and *egl-30*(*ad806*), FR reduced the mean velocity significantly (*Unpaired t-test*: both $p < 0.0001$) (Fig. 6a). In comparison, *egl-30*(*ad806*) had a significantly higher velocity than *egl-30*(*n686*) in the control experiment (*unpaired t-test*: 0.0168), which was in line with previous reports (Brundage et al., 1996). The spatial distribution of *egl-30*(*n686*) (*MBT*: $p < 0.0001$) and *egl-30*(*ad806*) (*MBT*: $p = 0.0003$) was affected significantly by FR (Fig. 6b). The results for both, *egl-30*(*n686*) and *egl-30*(*ad806*), were as expected, as the inhibition of G_q by FR increased their impairment leading to similar phenotypes as observed for *egl-30*(*ad805*).

The suppressor mutant *dgk-1*(*sy428*) depicted a significantly reduced velocity in presence of FR (*Mann-Whitney tests*: $p < 0.0001$) (Fig. 6a). This was expected as FR reduced G_q hyperactivity caused by the mutation *of dgk-1*. Compared to N2 in presence of FR *dgk-1*(*sy428*) had a significantly higher velocity in presence of FR (*Mann-Whitney test*: $p < 0.0001$) meaning that *dgk-1*(*sy428*) was able to rescue the velocity decrease by FR. The spatial distribution was significantly affected by FR, as less worms stayed inside the FR containing bacterial lawn (*MBT*: $p < 0.0001$) (Fig. 6b).

The suppressor mutant *eat-16*(*sa609*) displayed a slightly different picture, as there was a reduction of velocity, which was however not significant (*Multiple Mann-Whitney tests*: $p = 0.0534$). However, *eat-16*(*sa609*) grown in presence of FR was able to rescue the velocity decrease of N2 grown in presence of FR (*Mann-Whitney test*: $p < 0.0001$) as expected. Concerning spatial distribution, the number of

nematodes inside the lawn was significantly decreased in presence of FR (*MBT*: $p < 0.0001$) (Fig. 6). Compared to *dgk-1*(*sy428*) a greater span of velocities was observed for *eat-16*(*sa609*), which might be the reason for the lack of significance.

All nematodes, except the strong *egl-30*(*ad805*) mutant, seemed to avoid the presence of FR (Fig. 6b), as the number of nematodes was always significantly lower in the bacterial lawn with FR compared to the control. If *C. elegans* detects FR via its sensory system and initiates lawn avoidance as described for serrawettin W2, a cyclic depsipeptide and biosurfactant produced by *Serratia marcescens* Db10 (Pradel et al., 2007), it is likely that FR-Core would be detected similarly. However, experiments with FR-Core did not result in a changed spatial distribution of *C. elegans* N2 (Supplementary Tab. S2 of Online Resource 1), which suggests that avoidance is a result of FR's inhibitory effect. G_q signaling plays an antagonistic role in olfactory adaption to AWC-sensed odorants (Matsuki et al., 2006). Therefore, the G_q inhibition by FR might increase avoidance as nematodes would adapt faster. Nevertheless, as avoidance has been observed for all genotypes, except the strong mutant *egl-30*(*ad805*), the effect of FR is probably not solely connected to G_q inhibition. Further studies investigating a learned avoidance of FR by *C. elegans* might reveal new insights into the interaction of FR targets and FR producers.

As $G\alpha_q$ malfunction is associated with defective egg-laying (i.e., *egl*) by *C. elegans* (Brundage et al., 1996), we examined this in the presence of FR. In the respective set of experiments the strong *C. elegans egl-30*(*ad805*) mutant was not included, as time extended tracking experiments already had shown, as expected, that this mutant was not at all able to lay eggs (Supplementary Fig. S10 of Online Resource 1). To examine the egg-laying rate, all five genotypes (*C. elegans* N2, *C. elegans egl-30*(*n686*), *C. elegans egl-30*(*ad806*), *C. elegans dgk-1*(*sy428*), *C. elegans eat-16*(*sa609*)) were raised as described in the experimental section. Once they started to lay eggs, 12 nematodes per genotype and for each condition (i.e., with and without FR) were picked and placed on a new plate with the same condition (i.e., with or without FR). After two hours, nematodes were removed, and the eggs laid were counted.

According to literature, an adult hermaphrodite *C. elegans* lays between four to ten eggs per hour (Lints and Hall, 2004). This was confirmed during this experiment for the wildtype N2 with a mean of five eggs per hour (Fig. 7a). Unexpectedly, in the presence of FR the egg-laying rate of N2 slightly, but significantly increased (*Unpaired t-test*: $p = 0.0350$).

Mutation of *egl-30* result in egg-laying malfunction (Brundage et al., 1996), which was confirmed in our experiments (Fig. 7), as the weak *egl-30* mutants *egl-30*(*n686*) and *egl-30*(*ad806*) laid fewer eggs compared to wildtype. For both weak *egl-30* mutants, the egg-laying rate was significantly reduced (*Unpaired t-tests*: $p < 0.0001$, $p = 0.0005$) by FR treatment, and in the case of *egl-30*(*n686*) no eggs were laid, when FR was present. These results agree with the expected outcome, considering the influence of G_q on egg-laying.

The suppressor mutants *dgk-1*(*sy428*) and *eat-16*(*sa609*) showed reduced egg-laying compared to N2, which might be caused by the lack of egg production (Hajdu-Cronin et al., 1999). The suppressor

mutants, *dgk-1*(*sy428*) and *eat-16*(*sa609*) were not significantly affected by FR treatment (*Unpaired t-tests*: p = 0.3542, p = 0.0618).

Our results show that FR treatment caused a much more severe phenotype for the two weak *egl-30* mutants *egl-30*(*n686*) and *egl-30*(*ad806*). In addition, the two suppressor mutants *dgk-1*(*sy428*) and *eat-16*(*sa609*) were not affected by FR treatment, which was consistent with their known functions as suppressors of egl-30 mutants. However, it should be noted that FR treatment on N2 showed an unexpected result of increased egg-laying, possibly because of more eggs retained, or due to multifactorial influences.

A more common approach to investigate egg-laying defects is to count the numbers of eggs in the uterus. To disentangle the effects on egg-laying versus egg production, we performed the retained eggs assay and counted the number of eggs in the uterus of a worm, reasoning that the more eggs are still in the uterus, the lower must be the egg-laying rate. The weak *egl-30* mutants, *egl-30*(*n686*) and *egl-30*(*ad806*), were not evaluated again, due to the clear and unequivocal result in the egg-laying assay (Fig. 7a). To examine the number of retained eggs, nematodes were raised as detailed in the experimental section. After they reached the egg-laying adult stage, 20 worms per condition (i.e., with and without FR) and genotype (*C. elegans* N2, *C. elegans dgk-1*(*sy428*), *C. elegans eat-16*(*sa609*)) were picked and dissolved in bleach solution. Afterwards the remaining eggs were counted.

As depicted in Fig. 7b, wildtype N2 nematodes grown in presence of FR had significantly more eggs (*Unpaired t-test*: $p < 0.0001$) in their uterus. Untreated *eat-16*(*sa609*) and *dgk-1*(*sy428*) had a mean of 8 ± 1 eggs in their uterus. Prior reports had found fewer retained eggs, but used a different timing (Hajdu-Cronin et al., 1999). FR treatment increased the number of eggs in the mutants *dgk-1*(*sy428*) (*Mann-Whitney test*: p = 0.0012) and *eat-16*(*sa609*) (*Unpaired t-test*: p = 0.0005) as well. These results were as expected, as G_q inhibition by FR led to higher numbers of eggs in the uterus due to egg-laying inhibition. Additionally, both suppressor mutants were able to rescue N2 grown in presence of FR as the number of eggs in the uterus was significantly decreased by *dgk-1*(*sy428*) (Mann-Whitney test: $p < 0.0001$) and eat-16(sa609) (unpaired t-test: p = 0.0001).

Taken together, FR reduced velocity and inhibited egg-laying of *C. elegans.* Our results clearly show that FR targets the $G\alpha_q$ ortholog of *C. elegans* and leads to phenotypes as observed for *egl-30* deficient mutants.

FR reduces H. schachtii *J2 activity and inhibits hatching from cysts.* To assess the effect of FR on plant pathogenic nematodes, the cyst nematode *H. schachtii* was assayed *in vivo*. Parasitic cyst nematodes, e.g., *Globodera* and *Heterodera* spp., are difficult to erase from soil, as unhatched juvenile stage 2 worms (J2) can survive in the cyst for a long time. After hatching, J2 worms search the root of a plant which they penetrate, migrate into, and form a syncytium by modifying plant cells. Feeding on the syncytium, nematodes mature into the J4 stage for males or into adult stage for females. Fertilized females develop into the cysts. During the life cycle of *H. schachtii* only two stages are detached from the host plant, i.e.

the cyst and the J2 stage (Sijmons, 1993; Lilley et al., 2005; Bohlmann and Sobczak, 2014; Ngala et al., 2020).

Both J2´s and cysts were exposed to FR and moving *versus* nonmoving nematodes and hatched nematodes were counted respectively. The experiment with J2 stage nematodes was conducted with and without octopamine, which is used to stimulate feeding leading to an oral uptake of xenobiotic compounds from surrounding media (Urwin et al., 2002). Compared to the control, FR (without octopamine) significantly increased the number of inactive nematodes from 70–83% (*One-way ANOVA*: $p = 0.0009$). This effect was, however, even more pronounced in the presence of octopamine with only 9% inactive nematodes in the control and 92%, respectively in the presence of FR (*One-way ANOVA*: $p < 0.0001$). Octopamine alone significantly lowered the number of inactive nematodes in the control experiment from 70–9% (*One-way ANOVA*: $p < 0.0001$) and led to a significant increase of inactive worms in presence of FR from 83–92% (*One-way ANOVA*: $p = 0.0262$) (Fig. 8a). These observations were expected as octopamine increased the uptake of xenobiotic compounds like FR (Urwin et al., 2002) and significantly lowered the number of inactive nematodes in the control experiment due to its influence on movement (Masler, 2007) and quiescence (Griffin and Fitters, 2004; Schroeder and MacGuidwin, 2010). These results show that the inhibition of G_q by FR leads to a decreased activity of *H. schachtii* J2, the physiology behind this is however unknown.

Next, we investigated the concentration-dependency of this effect. As Fig. 8b depicts the number of inactive nematodes at the J2 stage is increasing in a FR concentration-dependent manner.

We then exposed cysts of *H. schachtii* to FR and counted the number of hatched juveniles in comparison to not treated cysts (Fig. 8c). FR inhibited hatching of J2, as the number of hatched J2 per cyst decreased in the presence of FR from 17 ± 1 to 7 ± 1 hatched J2 per cyst (*Unpaired t-test*: $p = 0.0002$).

Taken together, inhibition of G_q by FR leads to an inhibition of hatching from the cysts of *H. schachtii* J2. Hatching from cysts requires movement of the juvenile worms (Wallace, 1968) and since FR inhibits such activity, J2 may be unable to hatch. Other explanations are also possible, e.g., an influence of FR on the development of *H. schachtii* stages or inhibition of signaling cascades triggering hatching.

DISCUSSION

Microorganisms living in soil form an extremely complex microbiome, which plays a significant role in our ecosystem affecting the health of plants, animals and humans, one of the phenomena called “one health” (Banerjee and van der Heijden, 2023). The challenge to maintain a healthy and functioning soil microbiome depends on our knowledge of this complex system and its interactions (Jansson and Hofmockel, 2020; Banerjee and van der Heijden, 2023). Disease suppressive soils, in which fungi and bacteria cooperate to suppress plant parasitic nematodes demonstrate the beneficial interactions of the microbiome (Topalović et al., 2020). Research focusing on the soil microbiome is faced with an enormous complexity and huge gaps of knowledge (Fierer, 2017; Mishra et al., 2022). The herein

described investigation of the role of a bioactive natural product like FR and its microbial producer *C. vaccinii* contributes to decipher the complex puzzle of the soil microbiome.

C. vaccinii is not only producing FR, but also other secondary metabolites like the nonribosomal lipopeptides valhidepsins (Pistorius et al., 2023) and the purple pigment violacein (Soby et al., 2013). Valhidepsin-1 functions as surfactant (Pistorius et al., 2023) and may be required for the mobility of *C. vaccinii* on solid surfaces (Gutiérrez-Chávez et al., 2021). As the BGCs of valhidepsins and FR are co-localized, a synergistic effect in the ecological context is reasonable (Pistorius et al., 2023). Violacein itself is known as a quorum sensing indicator as the adaptive response triggered by the required quorum of bacteria leads to the production of this purple pigment (Durán et al., 2016; Park et al., 2021). Multiple biological effects of violacein have been investigated (Durán et al., 2021) including nematocidal activity (Ballestriero et al., 2014; Ballestriero et al., 2016). Synergistic experiments investigating the effect of these compounds together with FR may even more profoundly decipher the role of *C. vaccinii* in soil.

We herein present data showing that *C. vaccinii* is producing FR in soil-derived liquid media, i.e., SESOM from garden soil (Fig. 2a). However, the concentrations found in SESOM were low (around 0.0001 mg/mL) probably due to an insufficient mimicking of natural conditions. *C. vaccinii* was originally found near the root of cranberries (*Vaccinium macrocarpon* Ait) in bog soil (Soby et al., 2013), which consists of alternating layers of sand and organic matter supposedly with other nutrients than garden soil (Putnam et al., 2003). *C. vaccinii* might also be part of the rhizosphere of *V. macrocarpon* and therefore supplied with root exudates, which are lacking in SESOM. It also must be considered that multiple organisms are interacting in soil, inducing or inhibiting the production of metabolites. These interactions are difficult to simulate, but likely to influence FR production. The potential of *C. vaccinii* to produce higher amounts of FR is obvious from cultivations in LB medium, reaching levels of 2.5 mg/L (Hermes et al., 2021b). To answer the question on how much FR is really present in certain environments, an *in situ* approach would be of interest, in which a suitable adsorber resin is applied to extract FR from the respective surrounding (Kudela, 2011, 2017; Tuttle et al., 2019). A metagenomic analysis of environmental soil DNA for the *frs* BGC (Santana-Pereira et al., 2020) would yield novel data to judge the overall presence of potential FR producers. Still, though limited, our approach clearly indicates the ability of *C. vaccinii* to produce FR in soil.

FR is an inhibitor of G_q proteins involved in signal transduction of GPCRs and shown to have the potential to protect plants from insects (Crüsemann et al., 2018) and mammals (Miyamae et al., 1989; Matthey et al., 2017) *in vitro* and *in vivo*. Our *in silico* analysis of the putative FR-binding sites of various nematodic G_q proteins strongly indicated the possibility of FR-binding to an inhibition of these proteins. (Figs. 3 and 4). *In vitro* expression of *egl-30* (i.e. G_q) of *C. elegans* and the here newly identified $G\alpha_q$ ortholog of *H. schachtii* in HEK $G_{q/11}$-KO cells, together with overexpression of RIC-8A and M3, enabled functional expression and characterization of the proteins (Fig. 5). *In vitro*, FR inhibited both, *C. elegans* and *H. schachtii* $G\alpha_q$ signaling, as IP_1 accumulation and calcium increase were blocked.

In vivo, FR affects the nematode *C. elegans* by significantly decreasing their velocity (Fig. 6b) and inhibiting egg-laying (Fig. 7). Considering that *C. elegans* is feeding on bacteria, these effects suggest that *C. vaccinii* produces FR to reduce the activity and abundance of predators. *H. schachtii* is a pathogen feared in agricultural cultivation of crops belonging to the family Brassicaceae or Amaranthaceae, especially sugar beets (*Beta vulgaris*) (Daub, 2021), as the cysts persist in soil and are difficult to erase (Ngala et al., 2020). *In vivo* experiments (Fig. 8) demonstrate an inhibitory effect of FR on the activity of J2 *H. schachtii* and revealed FR to suppress hatching of J2.

It must be noted, however that the low concentrations of FR observed in SESOM could hardly lead to similar *in vivo* effects on *C. elegans* and *H. schachtii*. Chronic exposure to FR in soil and exponential effects (Chianese et al., 2018; Almasri et al., 2022) as conceivable by reduced egg-laying or hatching, could work together in a synergistic fashion. Also, a higher production of FR by *C. vaccinii* in soil compared to SESOM is reasonable. The presence of other potent metabolites from *C. vaccinii*, e.g., valhidepsins, for which a surfactant effect has been shown (Pistorius et al., 2023), and violacein (Soby et al., 2013), which is reported to have also nematocidal and antibacterial activity (Ballestriero et al., 2014) also has to be taken into account.

In this study, we provide one conclusive example for how, in the ecological context, the presence of bacteria like *C. vaccinii* and their excreted metabolome in the soil might contribute to an ecological equilibrium, being a prerequisite for the fruitful growth and cultivation of plants.

Declarations

Supplementary Information - The online version contains supplementary material available at xxx and xxx.

*Acknowledgment*s - We thank Dr. Sebastian Eves-van den Akker for access to the genome of *H. schachtii*. The Caenorhabditis Genetics Center, which is funded by NIH Office of Research Infrastructure Programs (P40 OD010440), provided some *C. elegans* strains. We thank the DBU (PhD scholarship 20018/568 to WH), the DFG (FOR 2372 grants KO 902/17-1 and 17-2 to GMK., FOR 2372 grants KO 1582/10-1 and 10-2 to EK, FOR2372 grant CR464/7-1 to MC and 214362475/GRK1873/2 funding JA), and the Max Planck Society (MS, JL) for funding.

Author Contributions - All authors contributed to the study conception and design. Soil sampling, *C. vaccinii* cultivation experiments, and *in silico* alignment were conducted and evaluated by WH. FR isolation was accomplished by SK. *In vitro* experiments and PyMOL comparisons, analyses, and figures were done by JA. WH, JL, and MS conducted and analyzed *in vivo* experiments with *C. elegans*. Experiments with *H. schachtii* were performed by PG and WH. Figures were arranged by WH. The first draft of manuscript was written by WH, supervised by GMK, and all authors read and approved the final manuscript.

Funding - Funding information is provided in acknowledgments.

Data availability - The data used to support the findings of this study are included in this article. The authors confirm that all other analyzed data and/or raw data generated during this study are available in supplementary information.

Conflict of Interest - All authors certify that they have no affiliations with or involvement in any organization or entity with any financial interest or non-financial interest in the subject matter or materials discussed in this manuscript.

References

1. Allan DB, Caswell T, Keim NC, van der Wel CM (2019) soft-matter/trackpy: Trackpy v0.4.2. Zenodo
2. Almasri H, Liberti J, Brunet J-L, Engel P, Belzunces LP (2022) Mild chronic exposure to pesticides alters physiological markers of honey bee health without perturbing the core gut microbiota. Sci Rep 12(1):4281. 10.1038/s41598-022-08009-2
3. Altschul SF, Madden TL, Schäffer AA, Zhang J et al (1997) Gapped BLAST and PSI-BLAST: a new generation of protein database search programs. Nucleic Acids Res 25 17:3389–3402. 10.1093/nar/25.17.3389
4. Altschul SF, Wootton JC, Gertz EM, Agarwala R et al (2005) Protein database searches using compositionally adjusted substitution matrices. FEBS J 272 20:5101–5109. 10.1111/j.1742-4658.2005.04945.x
5. Annala S, Feng X, Shridhar N, Eryilmaz F et al (2019) Direct targeting of Gαq and Gα11 oncoproteins in cancer cells. Sci Signal 12:573. 10.1126/scisignal.aau5948
6. Ballestriero F, Daim M, Penesyan A, Nappi J et al (2014) Antinematode activity of Violacein and the role of the insulin/IGF-1 pathway in controlling violacein sensitivity in Caenorhabditis elegans. PLoS ONE 9 10:e109201. 10.1371/journal.pone.0109201
7. Ballestriero F, Nappi J, Zampi G, Bazzicalupo P et al (2016) Caenorhabditis elegans employs innate and learned aversion in response to bacterial toxic metabolites tambjamine and violacein. Sci Rep 6:29284. 10.1038/srep29284
8. Banerjee S, van der Heijden MGA (2023) Soil microbiomes and one health. Nat Rev Microbiol 21 1:6–20. 10.1038/s41579-022-00779-w
9. Bardgett RD, van der Putten WH (2014) Belowground biodiversity and ecosystem functioning. Nature 515 7528:505–511. 10.1038/nature13855
10. Berendsen B, Pikkemaat M, Römkens P, Wegh R et al (2013) Occurrence of chloramphenicol in crops through natural production by bacteria in soil. J Agric Food Chem 61 17:4004–4010. 10.1021/jf400570c
11. Bohlmann H, Sobczak M (2014) The plant cell wall in the feeding sites of cyst nematodes. Front Plant Sci 5:89. 10.3389/fpls.2014.00089
12. Bonnard E, Liu J, Zjacic N, Alvarez L, Scholz M (2022) Automatically tracking feeding behavior in populations of foraging C. elegans

13. Brenner S (1974) The genetics of Caenorhabditis elegans. Genetics 77 1:71–94. 10.1093/genetics/77.1.71
14. Brundage L, Avery L, Katz A, Kim UJ et al (1996) Mutations in a C. elegans Gqalpha gene disrupt movement, egg laying, and viability. Neuron 16 5:999–1009. 10.1016/s0896-6273(00)80123-3
15. Carr R, Koziol-White C, Zhang J, Lam H et al (2016) Interdicting Gq Activation in Airway Disease by Receptor-Dependent and Receptor-Independent Mechanisms. Mol Pharmacol 89 1:94–104. 10.1124/mol.115.100339
16. Chan P, Thomas CJ, Sprang SR, Tall GG (2013) Molecular chaperoning function of Ric-8 is to fold nascent heterotrimeric G protein α subunits. Proc Natl Acad Sci U S A 110 10:3794–3799. 10.1073/pnas.1220943110
17. Chianese R, Viggiano A, Urbanek K, Cappetta D et al (2018) Chronic exposure to low dose of bisphenol A impacts on the first round of spermatogenesis via SIRT1 modulation. Sci Rep 8(1):2961. 10.1038/s41598-018-21076-8
18. Crüsemann M, Reher R, Schamari I, Brachmann AO et al (2018) Heterologous Expression, Biosynthetic Studies, and Ecological Function of the Selective Gq-Signaling Inhibitor FR900359. Angew Chem Int Ed Engl 57 3:836–840. 10.1002/anie.201707996
19. Daub M (2021) The beet cyst nematode (Heterodera schachtii): an ancient threat to sugar beet crops in Central Europe has become an invisible actor. In: Sikora RA, Desaeger J, Molendijk L (eds) Integrated nematode management: state-of-the-art and visions for the future. CABI, UK, pp 394–399
20. Davis P, Zarowiecki M, Arnaboldi V, Becerra A et al (2022) WormBase in 2022-data, processes, and tools for analyzing Caenorhabditis elegans. Genetics 220:4. 10.1093/genetics/iyac003
21. Dillman AR, Sternberg PW (2012) Entomopathogenic nematodes. Curr Biol 22 11:R430–R431. 10.1016/j.cub.2012.03.047
22. Downes GB, Gautam N (1999) The G protein subunit gene families. Genomics 62 3:544–552. 10.1006/geno.1999.5992
23. Durán N, Justo GZ, Durán M, Brocchi M et al (2016) Advances in Chromobacterium violaceum and properties of violacein-Its main secondary metabolite: A review. Biotechnol Adv 34 5:1030–1045. 10.1016/j.biotechadv.2016.06.003
24. Durán N, Nakazato G, Durán M, Berti IR et al (2021) Multi-target drug with potential applications: violacein in the spotlight. World J Microbiol Biotechnol 37 9:151. 10.1007/s11274-021-03120-4
25. Ferris H (2010) Contribution of nematodes to the structure and function of the soil food web. J Nematol 42 1:63–67
26. Fierer N (2017) Embracing the unknown: disentangling the complexities of the soil microbiome. Nat Rev Microbiol 15 10:579–590. 10.1038/nrmicro.2017.87
27. Flock T, Ravarani CNJ, Sun D, Venkatakrishnan AJ et al (2015) Universal allosteric mechanism for Gα activation by GPCRs. Nature 524 7564:173–179. 10.1038/nature14663

28. Fujioka M, Koda S, Morimoto Y, Biemann K (1988) Structure of FR900359, a cyclic depsipeptide from Ardisia crenata sims. J Org Chem 53 12:2820–2825. 10.1021/jo00247a030
29. Griffin C, Fitters P (2004) Spontaneous and induced activity of Heterorhabditis megidis infective juveniles during storage. Nematol 6 6:911–917. 10.1163/1568541044038597
30. Gutbrod P, Gutbrod K, Nauen R, Elashry A et al (2020) Inhibition of acetyl-CoA carboxylase by spirotetramat causes growth arrest and lipid depletion in nematodes. Sci Rep 10 1:12710. 10.1038/s41598-020-69624-5
31. Gutiérrez-Chávez C, Benaud N, Ferrari BC (2021) The ecological roles of microbial lipopeptides: Where are we going? Comput Struct Biotechnol J 19:1400–1413. 10.1016/j.csbj.2021.02.017
32. Hajdu-Cronin YM, Chen WJ, Patikoglou G, Koelle MR, Sternberg PW (1999) Antagonism between G(o)alpha and G(q)alpha in Caenorhabditis elegans: the RGS protein EAT-16 is necessary for G(o)alpha signaling and regulates G(q)alpha activity. Genes Dev 13 14:1780–1793. 10.1101/gad.13.14.1780
33. Harris TW, Arnaboldi V, Cain S, Chan J et al (2020) WormBase: a modern Model Organism Information Resource. Nucleic Acids Res 48 D1:D762–D767. 10.1093/nar/gkz920
34. Hermes C, König GM, Crüsemann M (2021a) The chromodepsins - chemistry, biology and biosynthesis of a selective Gq inhibitor natural product family. Nat Prod Rep 38 12:2276–2292. 10.1039/D1NP00005E
35. Hermes C, Richarz R, Wirtz DA, Patt J et al (2021b) Thioesterase-mediated side chain transesterification generates potent Gq signaling inhibitor FR900359. Nat Commun 12:1. 10.1038/s41467-020-20418-3
36. Himmelreich S, Masuho I, Berry JA, MacMullen C et al (2017) Dopamine Receptor DAMB Signals via Gq to Mediate Forgetting in Drosophila. Cell Rep 21 8:2074–2081. 10.1016/j.celrep.2017.10.108
37. Ingham RE, Trofymow JA, Ingham ER, Coleman DC (1985) Interactions of Bacteria, Fungi, and their Nematode Grazers: Effects on Nutrient Cycling and Plant Growth. Ecol Monogr 55 1:119–140. 10.2307/1942528
38. Insel PA, Sriram K, Gorr MW, Wiley SZ et al (2019) GPCRomics: An Approach to Discover GPCR Drug Targets. Trends Pharmacol Sci 40 6:378–387. 10.1016/j.tips.2019.04.001
39. Jansson JK, Hofmockel KS (2020) Soil microbiomes and climate change. Nat Rev Microbiol 18 1:35–46. 10.1038/s41579-019-0265-7
40. Jose AM, Koelle MR (2005) Domains, amino acid residues, and new isoforms of Caenorhabditis elegans diacylglycerol kinase 1 (DGK-1) important for terminating diacylglycerol signaling in vivo. J Biol Chem 280 4:2730–2736. 10.1074/jbc.M409460200
41. Kamato D, Mitra P, Davis F, Osman N et al (2017) Gaq proteins: molecular pharmacology and therapeutic potential. Cell Mol Life Sci 74 8:1379–1390. 10.1007/s00018-016-2405-9
42. Kenney E, Eleftherianos I (2016) Entomopathogenic and plant pathogenic nematodes as opposing forces in agriculture. Int J Parasitol 46 1:13–19. 10.1016/j.ijpara.2015.09.005

43. Klepac K, Kilić A, Gnad T, Brown LM et al (2016) The Gq signalling pathway inhibits brown and beige adipose tissue. Nat Commun 7:10895. 10.1038/ncomms10895
44. Koppenhöfer AM, Shapiro-Ilan DI, Hiltpold I (2020) Entomopathogenic Nematodes in Sustainable Food Production. Front Sustain Food Syst 4. 10.3389/fsufs.2020.00125
45. Kostenis E, Pfeil EM, Annala S (2020) Heterotrimeric Gq proteins as therapeutic targets? J Biol Chem 295 16:5206–5215. 10.1074/jbc.REV119.007061
46. Kouser Y, Shah AA, Rasmann S (2021) The functional role and diversity of soil nematodes are stronger at high elevation in the lesser Himalayan Mountain ranges. Ecol Evol 11 20:13793–13804. 10.1002/ece3.8061
47. Kudela RM (2011) Characterization and deployment of Solid Phase Adsorption Toxin Tracking (SPATT) resin for monitoring of microcystins in fresh and saltwater. Harmful Algae 11:117–125. 10.1016/j.hal.2011.08.006
48. Kudela RM (2017) Passive Sampling for Freshwater and Marine Algal Toxins, pp. 379–409. in Recent Advances in the Analysis of Marine Toxins. Elsevier
49. Kuschak M, Namasivayam V, Rafehi M, Voss JH et al (2019) Cell-permeable high-affinity tracers for Gq proteins provide structural insights, reveal distinct binding kinetics, and identify small molecule inhibitors. Br J Pharmacol. 10.1111/bph.14960
50. Lapadula D, Farias E, Randolph CE, Purwin TJ et al (2019) Effects of Oncogenic Gαq and Gα11 Inhibition by FR900359 in Uveal Melanoma. Mol Cancer Res 17 4:963–973. 10.1158/1541-7786.MCR-18-0574
51. Lazarova S, Coyne D, Rodríguez G, Peteira MG, B., and, Ciancio A (2021) Functional Diversity of Soil Nematodes in Relation to the Impact of Agriculture—A Review. Diversity 13 2:64. 10.3390/d13020064
52. Lilley CJ, Atkinson HJ, Urwin PE (2005) Molecular aspects of cyst nematodes. Mol Plant Pathol 6 6:577–588. 10.1111/J.1364-3703.2005.00306.X
53. Lints R, Hall DH (2004) WormAtlas Hermaphrodite Handbook - Reproductive System - Egg-laying Apparatus. WormAtlas. 10.3908/wormatlas.1.24
54. Lokits AD, Indrischek H, Meiler J, Hamm HE, Stadler PF (2018) Tracing the evolution of the heterotrimeric G protein α subunit in Metazoa. BMC Evol Biol 18:151. 10.1186/s12862-018-1147-8
55. Malfacini D, Patt J, Annala S, Harpsøe K et al (2019) Rational design of a heterotrimeric G protein α subunit with artificial inhibitor sensitivity. J Biol Chem 294 15:5747–5758. 10.1074/jbc.RA118.007250
56. Masler EP (2007) Responses of Heterodera glycines and Meloidogyne incognita to exogenously applied neuromodulators. J Helminthol 81 4:421–427. 10.1017/S0022149X07850243
57. Matsuki M, Kunitomo H, Iino Y (2006) Goalpha regulates olfactory adaptation by antagonizing Gqalpha-DAG signaling in Caenorhabditis elegans. Proc Natl Acad Sci U S A 103 4:1112–1117. 10.1073/pnas.0506954103

58. Matthey M, Roberts R, Seidinger A, Simon A et al (2017) Targeted inhibition of Gq signaling induces airway relaxation in mouse models of asthma. Sci Transl Med 9:407. 10.1126/scitranslmed.aag2288
59. Melakeberhan H, Bonito G, Kravchenko AN (2021) Application of Nematode Community Analyses-Based Models towards Identifying Sustainable Soil Health Management Outcomes: A Review of the Concepts. Soil Syst 5 2:32. 10.3390/soilsystems5020032
60. Meleka MM, Edwards AJ, Xia J, Dahlen SA et al (2019) Anti-hypertensive mechanisms of cyclic depsipeptide inhibitor ligands for Gq/11 class G proteins. Pharmacol Res 141:264–275. 10.1016/j.phrs.2019.01.012
61. de Mendoza A, Sebé-Pedrós A, Ruiz-Trillo I (2014) The evolution of the GPCR signaling system in eukaryotes: modularity, conservation, and the transition to metazoan multicellularity. Genome Biol Evol 6 3:606–619. 10.1093/gbe/evu038
62. Miller KG, Emerson MD, McManus JR, Rand JB (2000) RIC-8 (Synembryn): a novel conserved protein that is required for G(q)alpha signaling in the C. elegans nervous system. Neuron 27 2:289–299. 10.1016/s0896-6273(00)00037-4
63. Miller KG, Emerson MD, Rand JB (1999) Goα and Diacylglycerol Kinase Negatively Regulate the Gqα Pathway in C. elegans. Neuron 24 2:323–333. 10.1016/s0896-6273(00)80847-8
64. Mishra A, Singh L, Singh D (2022) Unboxing the black box-one step forward to understand the soil microbiome: A systematic review. Microb Ecol. 10.1007/s00248-022-01962-5
65. Miyamae A, Fujioka M, Koda S, Morimoto Y (1989) Structural studies of FR900359, a novel cyclic depsipeptide from Ardisia crenata sims(Myrsinaceae). J Chem Soc Perkin Trans 1 5:873. 10.1039/P19890000873
66. Ngala B, Mariette N, Ianszen M, Dewaegeneire P et al (2020) Hatching Induction of Cyst Nematodes in Bare Soils Drenched With Root Exudates Under Controlled Conditions. Front Plant Sci 11:602825. 10.3389/fpls.2020.602825
67. Nishimura A, Kitano K, Takasaki J, Taniguchi M et al (2010) Structural basis for the specific inhibition of heterotrimeric Gq protein by a small molecule. Proc Natl Acad Sci U S A 107 31:13666–13671. 10.1073/pnas.1003553107
68. Onken MD, Noda SE, Kaltenbronn KM, Frankfater C et al (2022) Oncogenic Gq/11 signaling acutely drives and chronically sustains metabolic reprogramming in uveal melanoma. J Biol Chem 298 1:101495. 10.1016/j.jbc.2021.101495
69. Park H, Park S, Yang Y-H, Choi K-Y (2021) Microbial synthesis of violacein pigment and its potential applications. Crit Rev Biotechnol 41 6:879–901. 10.1080/07388551.2021.1892579
70. Patt J, Alenfelder J, Pfeil EM, Voss JH et al (2021) An experimental strategy to probe Gq contribution to signal transduction in living cells. J Biol Chem 296:100472. 10.1016/j.jbc.2021.100472
71. Pistorius D, Buntin K, Richard E, Rust M et al (2023) Valhidepsin Lipopeptides from Chromobacterium vaccinii: Structures, Biosynthesis, and Coregulation with FR900359 Production. J Nat Prod. 10.1021/acs.jnatprod.2c00825

72. Porazinska DL, Giblin-Davis RM, Faller L, Farmerie W et al (2009) Evaluating high-throughput sequencing as a method for metagenomic analysis of nematode diversity. Mol Ecol Resour 9 6:1439–1450. 10.1111/j.1755-0998.2009.02611.x
73. Pradel E, Zhang Y, Pujol N, Matsuyama T et al (2007) Detection and avoidance of a natural product from the pathogenic bacterium Serratia marcescens by Caenorhabditis elegans. Proc Natl Acad Sci U S A 104 7:2295–2300. 10.1073/pnas.0610281104
74. Procter DL (1990) Global Overview of the Functional Roles of Soil-living Nematodes in Terrestrial Communities and Ecosystems. J Nematol 22 1:1–7
75. Putnam RA, Nelson JO, Clark JM (2003) The persistence and degradation of chlorothalonil and chlorpyrifos in a cranberry bog. J Agric Food Chem 51 1:170–176. 10.1021/jf020744r
76. Santana-Pereira ALR, Sandoval-Powers M, Monsma S, Zhou J et al (2020) Discovery of Novel Biosynthetic Gene Cluster Diversity From a Soil Metagenomic Library. Front Microbiol 11:585398. 10.3389/fmicb.2020.585398
77. Schneider CA, Rasband WS, Eliceiri KW (2012) NIH Image to ImageJ: 25 years of image analysis. Nat Methods 9 7:671–675. 10.1038/nmeth.2089
78. Schrage R, Schmitz A-L, Gaffal E, Annala S et al (2015) The experimental power of FR900359 to study Gq-regulated biological processes. Nat Commun 6:10156. 10.1038/ncomms10156
79. Schroeder NE, MacGuidwin AE (2010) Behavioural quiescence reduces the penetration and toxicity of exogenous compounds in second-stage juveniles of Heterodera glycines. Nematol 12 2:277–287. 10.1163/138855409X12506855979712
80. Siddique S, Radakovic ZS, Hiltl C, Pellegrin C et al (2022) The genome and lifestage-specific transcriptomes of a plant-parasitic nematode and its host reveal susceptibility genes involved in trans-kingdom synthesis of vitamin B5. Nat Commun 13 1:6190. 10.1038/s41467-022-33769-w
81. Sijmons PC (1993) Plant-nematode interactions. Plant Mol Biol 23 5:917–931. 10.1007/BF00021809
82. Sijmons PC, Grundler FM, Mende N, Burrows PR, Wyss U (1991) Arabidopsis thaliana as a new model host for plant-parasitic nematodes. Plant J 1 2:245–254. 10.1111/j.1365-313X.1991.00245.x
83. Singh S, Singh B, Singh AP (2015) Nematodes: A Threat to Sustainability of Agriculture. Procedia Environ Sci 29:215–216. 10.1016/j.proenv.2015.07.270
84. Soby SD, Gadagkar SR, Contreras C, Caruso FL (2013) Chromobacterium vaccinii sp. nov., isolated from native and cultivated cranberry (Vaccinium macrocarpon Ait.) bogs and irrigation ponds. Int J Syst Evol Microbiol 63 Pt 5:1840–1846. 10.1099/ijs.0.045161-0
85. Song D, Pan K, Tariq A, Sun F et al (2017) Large-scale patterns of distribution and diversity of terrestrial nematodes. Appl Soil Ecol 114:161–169. 10.1016/j.apsoil.2017.02.013
86. Tall GG, Krumins AM, Gilman AG (2003) Mammalian Ric-8A (synembryn) is a heterotrimeric Galpha protein guanine nucleotide exchange factor. J Biol Chem 278 10:8356–8362. 10.1074/jbc.M211862200

87. Taniguchi M, Nagai K, Arao N, Kawasaki T et al (2003a) YM-254890, a novel platelet aggregation inhibitor produced by Chromobacterium sp. QS3666. J Antibiot (Tokyo) 56 4:358–363. 10.7164/antibiotics.56.358
88. Taniguchi M, Suzumura K, Nagai K, Kawasaki T et al (2003b) Structure of YM-254890, a Novel Gq/11 Inhibitor from Chromobacterium sp. QS3666. Tetrahedron 59 25:4533–4538. 10.1016/S0040-4020(03)00680-X
89. Topalović O, Hussain M, Heuer H (2020) Plants and Associated Soil Microbiota Cooperatively Suppress Plant-Parasitic Nematodes. Front Microbiol 11:313. 10.3389/fmicb.2020.00313
90. Trap J, Bonkowski M, Plassard C, Villenave C, Blanchart E (2016) Ecological importance of soil bacterivores for ecosystem functions. Plant Soil 398(1–2):1–24. 10.1007/s11104-015-2671-6
91. Tuttle RN, Demko AM, Patin NV, Kapono CA et al (2019) Detection of Natural Products and Their Producers in Ocean Sediments. Appl Environ Microbiol 85:8. 10.1128/AEM.02830-18
92. Urwin PE, Lilley CJ, Atkinson HJ (2002) Ingestion of double-stranded RNA by preparasitic juvenile cyst nematodes leads to RNA interference. Mol Plant Microbe Interact 15 8:747–752. 10.1094/MPMI.2002.15.8.747
93. van den Hoogen J, Geisen S, Routh D, Ferris H et al (2019) Soil nematode abundance and functional group composition at a global scale. Nature 572 7768:194–198. 10.1038/s41586-019-1418-6
94. van Pham HT, Kim J (2012) Cultivation of unculturable soil bacteria. Trends Biotechnol 30 9:475–484. 10.1016/j.tibtech.2012.05.007
95. Vilain S, Luo Y, Hildreth MB, Brözel VS (2006) Analysis of the life cycle of the soil saprophyte Bacillus cereus in liquid soil extract and in soil. Appl Environ Microbiol 72 7:4970–4977. 10.1128/AEM.03076-05
96. Vöing K, Harrison A, Soby SD (2015) Draft Genome Sequence of Chromobacterium vaccinii, a Potential Biocontrol Agent against Mosquito (Aedes aegypti) Larvae. Genome Announc 3:3. 10.1128/genomeA.00477-15
97. Voss JH, Nagel J, Rafehi M, Guixà-González R et al (2021) Unraveling binding mechanism and kinetics of macrocyclic Gαq protein inhibitors. Pharmacol Res 173:105880. 10.1016/j.phrs.2021.105880
98. Wallace HR (1968) Undulatory locomotion of the plant parasitic nematode Meloidogyne javanica. Parasitology 58 2:377–391. 10.1017/S0031182000069419
99. Wong K-F, Wong W-K, Lin M-S (2014) Forward selection two sample binomial test. J Data Sci 12 4:279–294
100. Xiong X-F, Zhang H, Boesgaard MW, Underwood CR et al (2019) Structure-Activity Relationship Studies of the Natural Product Gq/11 Protein Inhibitor YM-254890. ChemMedChem 14 8:865–870. 10.1002/cmdc.201900018
101. Xiong X-F, Zhang H, Underwood CR, Harpsøe K et al (2016) Total synthesis and structure-activity relationship studies of a series of selective G protein inhibitors. Nat Chem 8 11:1035–1041. 10.1038/nchem.2577

102. Yamashita J, Nakao Y, Katsumata R (2011) WO 2011/142485 A1
103. Yeates GW, Bongers T, de Goede RG, Freckman DW, Georgieva SS (1993) Feeding habits in soil nematode families and genera-an outline for soil ecologists. J Nematol 25 3:315–331
104. Zhang H, Nielsen AL, Boesgaard MW, Harpsøe K et al (2018) Structure-activity relationship and conformational studies of the natural product cyclic depsipeptides YM-254890 and FR900359. Eur J Med Chem 156:847–860. 10.1016/j.ejmech.2018.07.023

Figures

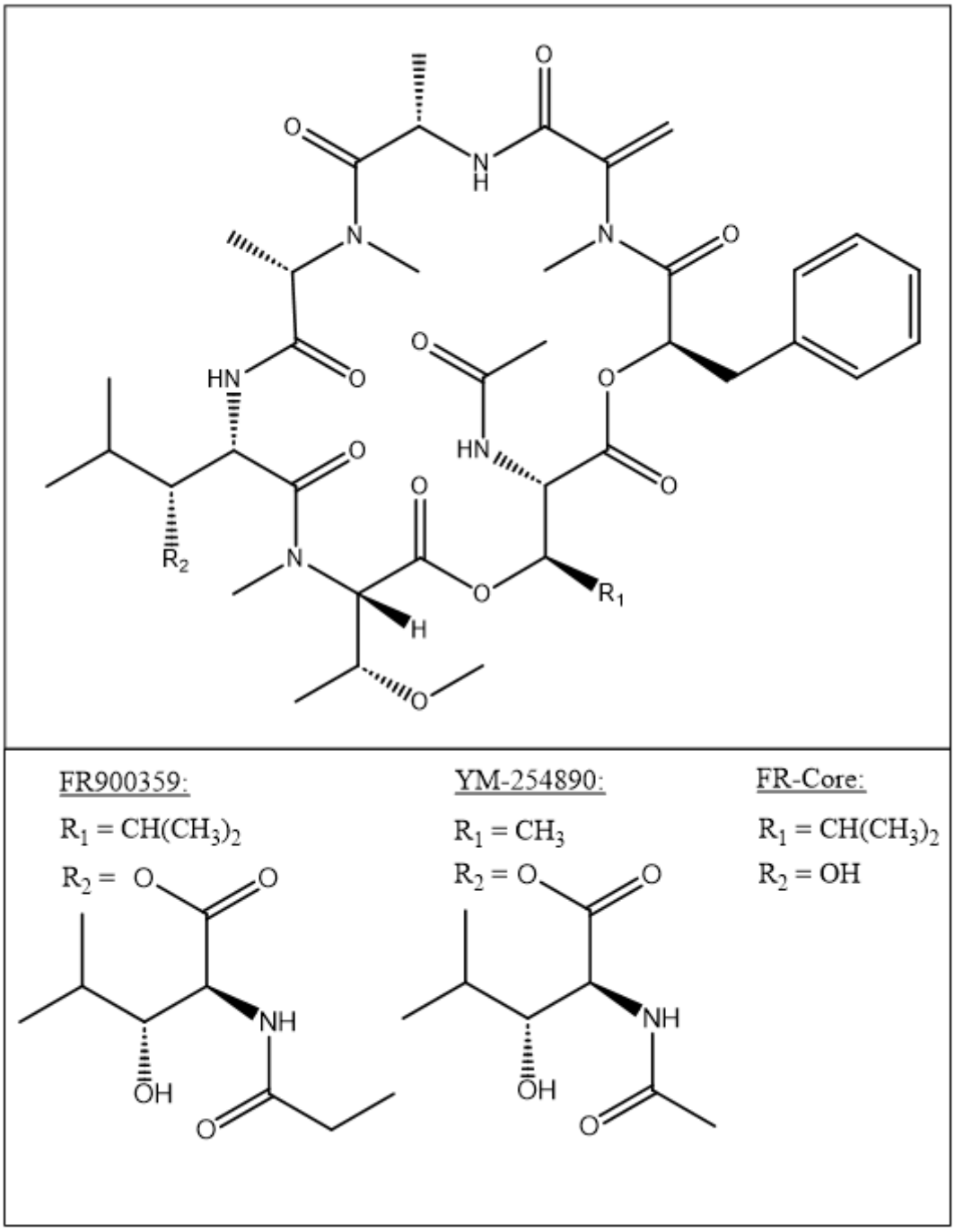

Figure 1

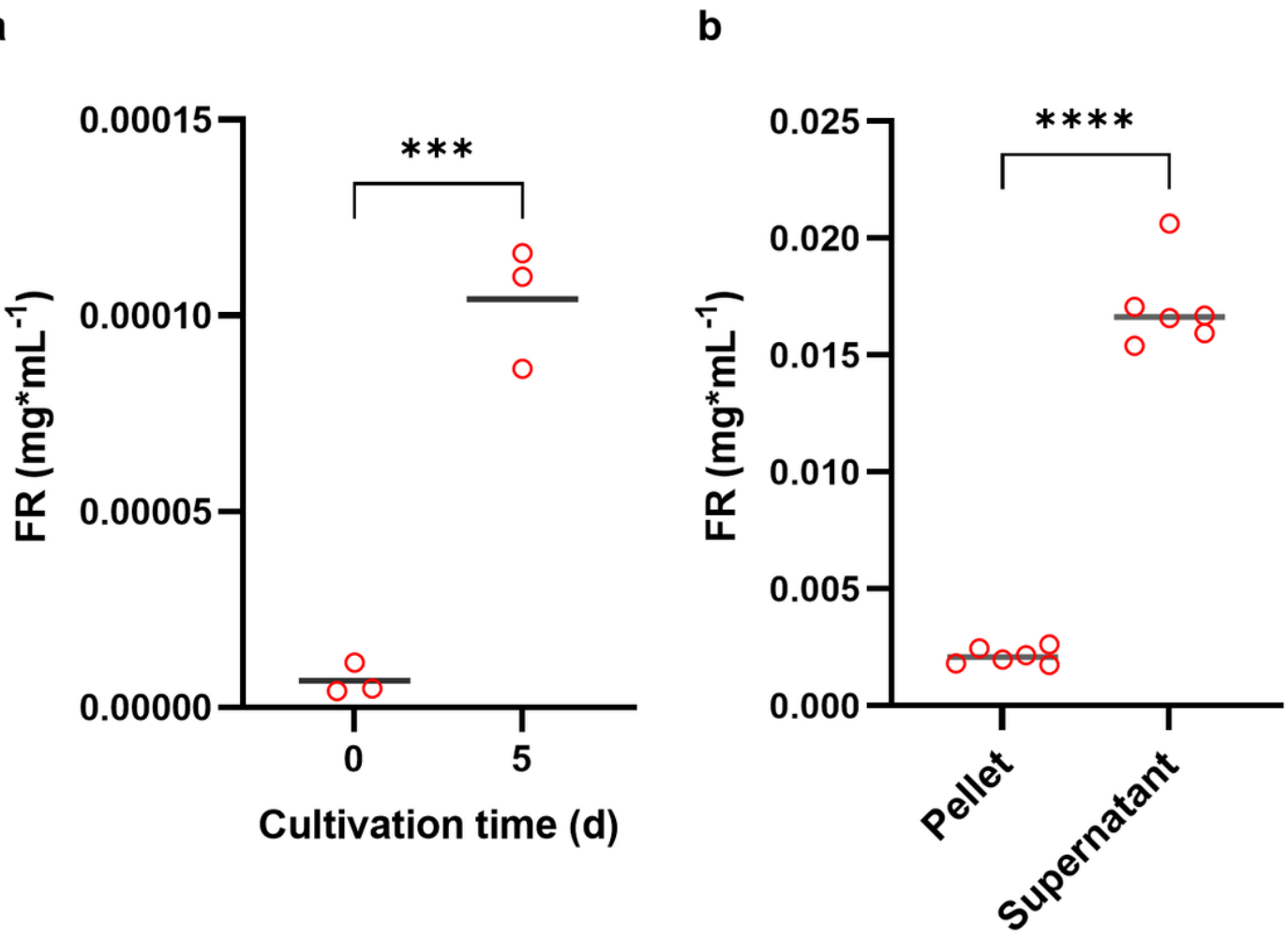

Figure 2

a FR concentration as determined after n-butanol extraction of a C. vaccinii culture in SESOM, cultivated for 5 days or extracted after inoculation (0 days). FR concentration was evaluated using HPLC/MS. For both experiments, n=3. The significance was determined using a two-tailed unpaired t-test. **b** Concentration of FR (mg/mL) in supernatant and pellet of C. vaccinii liquid culture. C. vaccinii was cultivated for 43 h in LB medium and centrifuged afterwards, resulting in pellet and supernatant, which were extracted separately with n-butanol. Six repeats were performed. The significance was determined using a paired t-test. $P > 0.05$ = ns, $P < 0.05$ = *, $P < 0.01$ = **, $P < 0.001$ = ***, $P < 0.0001$ = ****

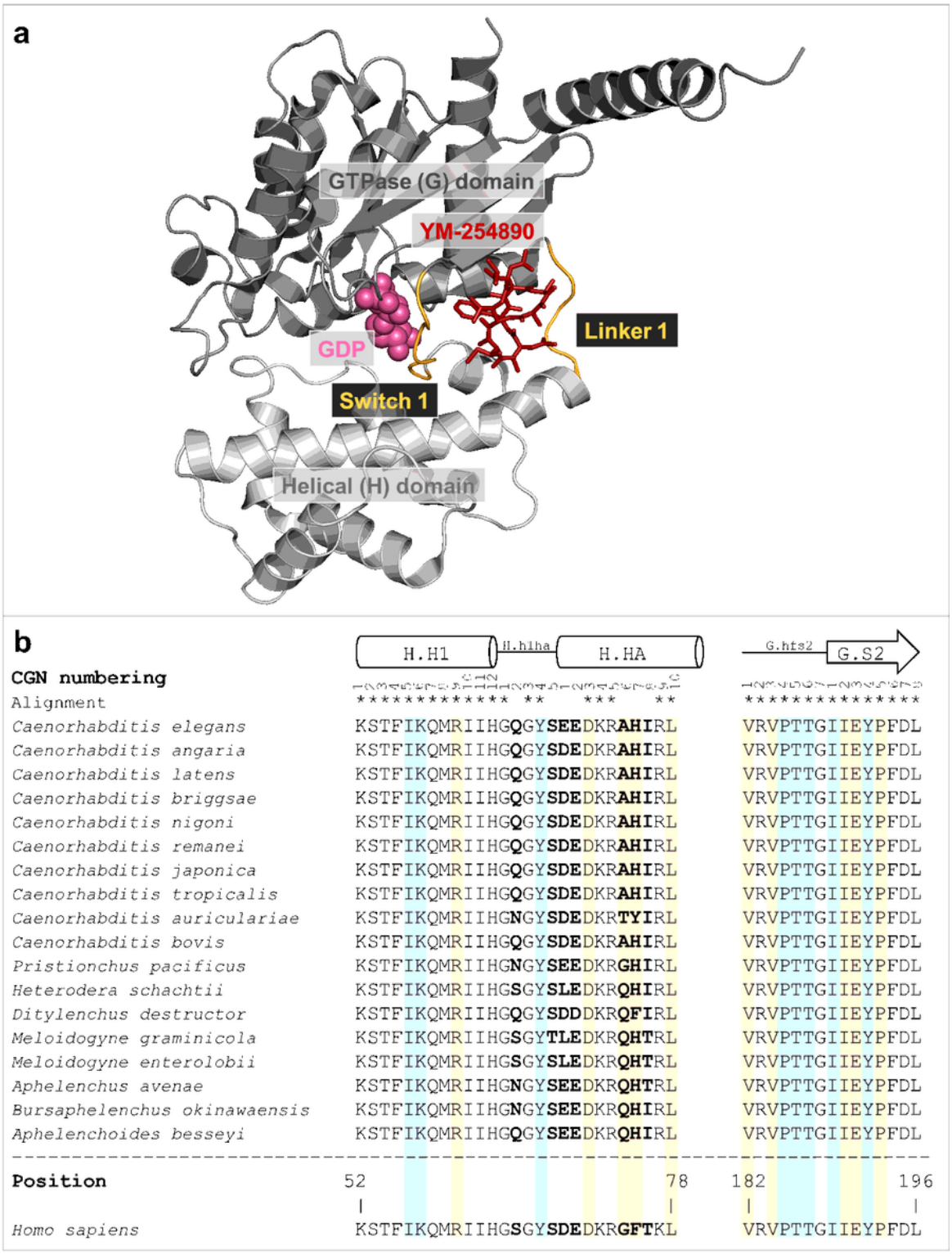

Figure 3

a $G\alpha_{i/q}\beta\gamma$ heterotrimer (grey) in complex with YM-254890 (red, sticks) and guanosine diphosphate (spheres, rose) (PDB Code: 3AH8). Linker 1 and switch I (linker 2) are shown in orange. **b** FR- and YM-binding sites in $G\alpha_q$ proteins of nematodes. Sequences (Supplementary Tab. S1 of Online Resource 1) were aligned using the Clustal W algorithm and compared to the human $G\alpha_q$ protein (UniProtKB: P50148). Identical positions within the binding sites are marked with asterisks and positions shown in

bold are divergent. Positions predicted to be important for FR- and YM-binding are highlighted in blue, and positions confirmed via mutagenesis studies highlighted in orange . The $G\alpha_q$ nomenclature from CGN was used and secondary structures were indicated with symbols (cylinder=α-helix; arrow=β-sheet)

(Nishimura et al., 2010; Malfacini et al., 2019; Voss et al., 2021)

(Flock et al., 2015)

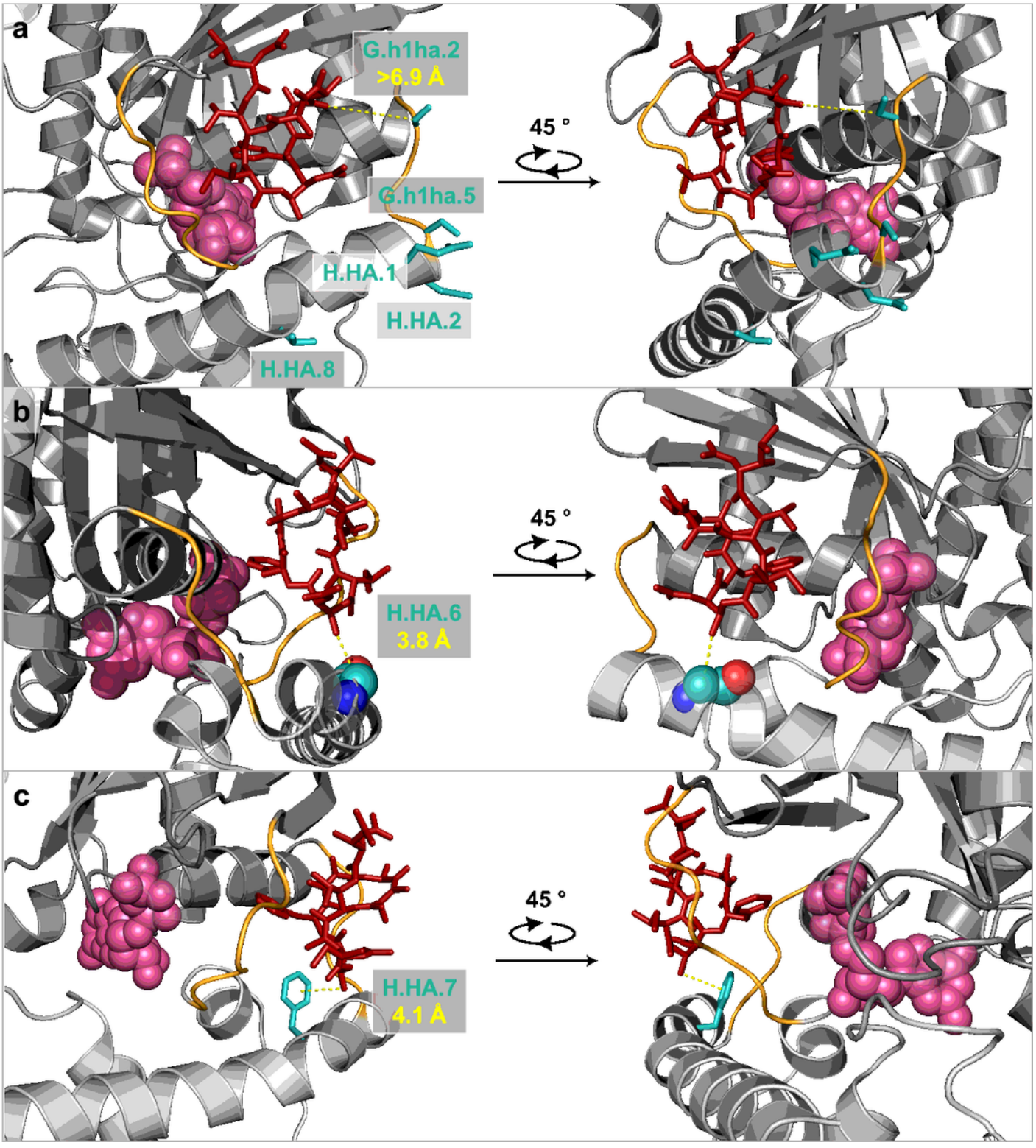

Figure 4

$G\alpha_{i/q}\beta\gamma$ heterotrimer (grey) in complex with YM-254890 (red, sticks) and guanosine diphosphate (spheres, rose) (PDB Code: 3AH8). Linker 1 and switch I (linker 2) are shown in orange. Representation of human residues at positions with differing nematode amino acids in the $G\alpha_q$ sequence alignment $S65^{G.h1ha.2}$, $S68^{G.h1ha.5}$, $D69^{H.HA.1}$, $E70^{H.HA.2}$, and $T76^{H.HA.8}$ in **a** as turquoise sticks; $G74^{H.HA.6}$ in **b** as spheres; $F75^{H.HA.7}$ in **c** as turquoise sticks. Each position was rotated once by 45° along the z-axis. Measured distances between the amino acids and YM are shown as dashed yellow lines. Visualization and measurement were done using PyMOL™ 2.5.4 [CAVE: Noch nicht von Prof. Kostenis durchgesehen/Not yet reviewed by Prof. Kostenis]

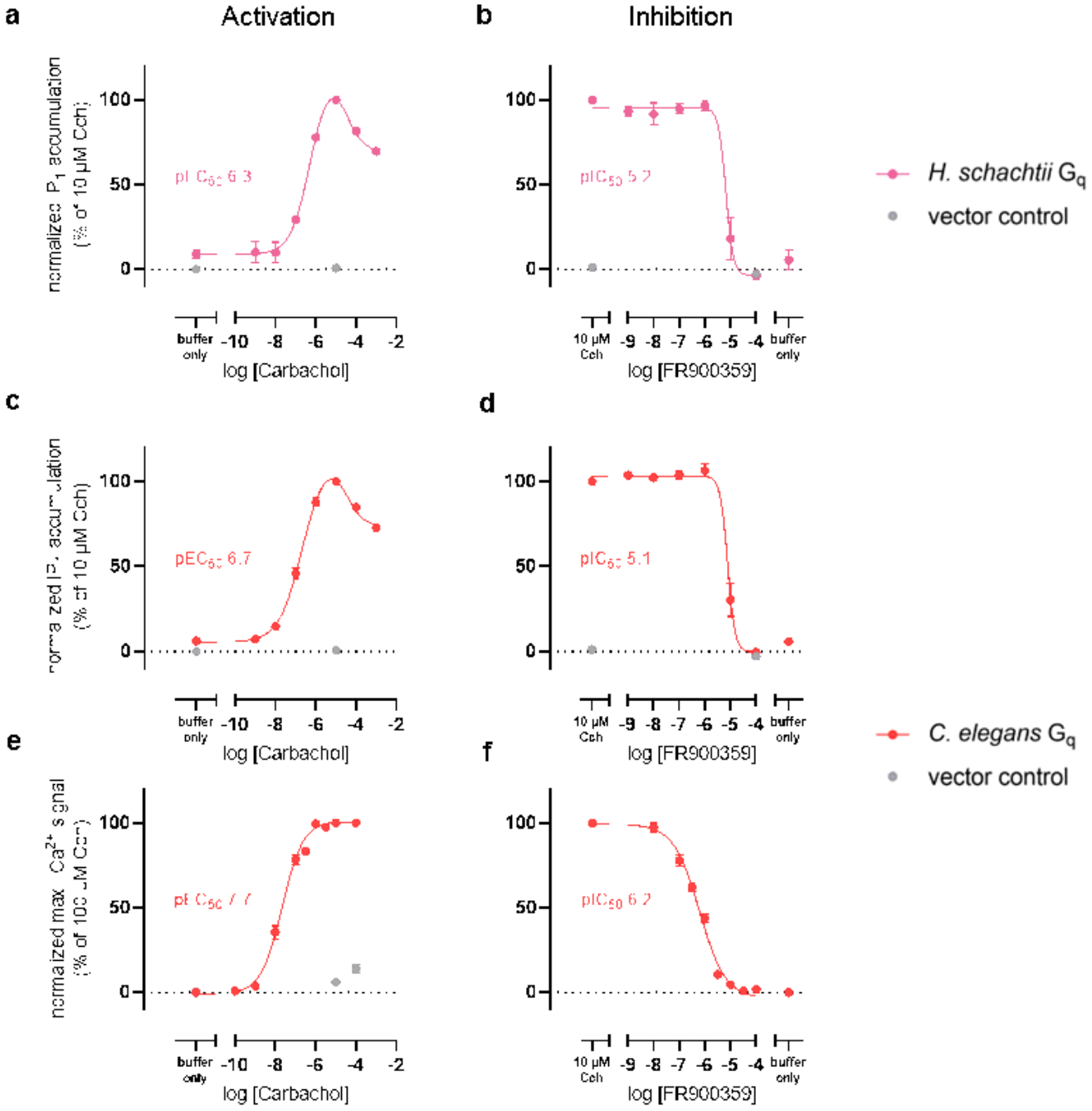

Figure 5

Functional expression of nematode $G\alpha_q$ proteins and inhibition by FR. **a**, **c** Concentration-dependent IP_1 accumulation after stimulation of HEK293 $G\alpha_q/G\alpha_{11}$-null cells transfected to express **a** H. schachtii and **c** C. elegans $G\alpha_q$ isoforms with carbachol. **b**, **d** Concentration-inhibition curves of FR on H. schachtii **b** and C. elegans **c** $G\alpha_q$ proteins normalized to the IP_1 accumulation evoked by 10 µM carbachol. **e** Concentration-dependent calcium signal after stimulation of HEK293 $G\alpha_q/G\alpha_{11}$-null cells transfected to express C. elegans $G\alpha_q$ isoforms with carbachol. **f** Concentration-inhibition curves of FR on C. elegans $G\alpha_q$ proteins normalized to the calcium signal evoked by 100 µM carbachol. Mean +/- SEM, at least 3 biological replicates performed in triplicate

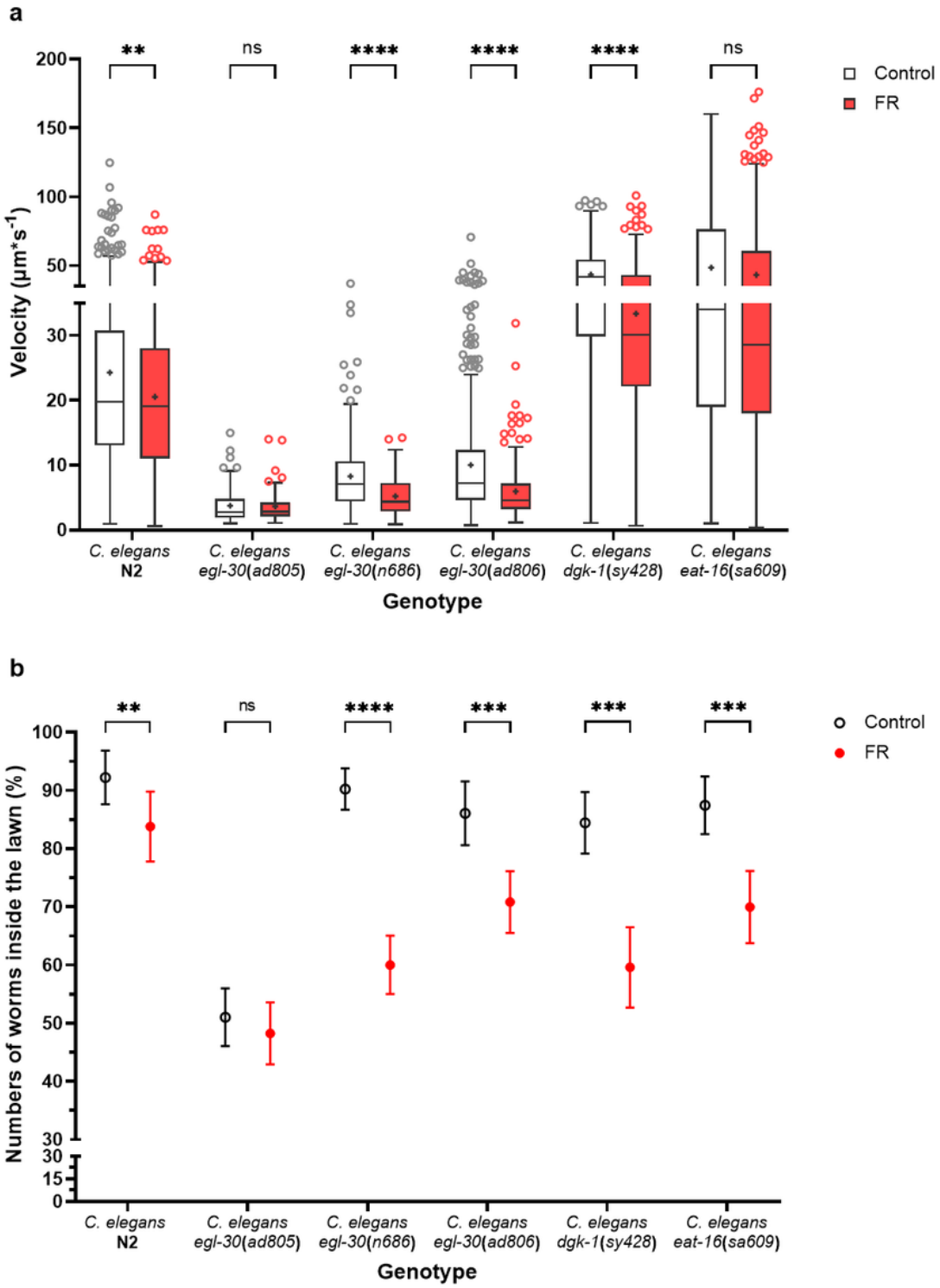

Figure 6

Effect of FR on velocity **a** and spatial distribution **b** of six C. elegans genotypes (N2, egl-30(ad805), egl-30(n686), egl-30(ad806), dgk-1(sy428), eat-16(sa609)). All nematodes were fed with E. coli OP50, placed as lawn in the middle of the NGM plate and mixed with 1% DMSO (Control). In the FR group 2.5 mM FR were added to the food. The movement of adult nematodes in and around the lawn was recorded and analyzed. Velocities are displayed as box plot with Tukey whiskers (Quartile ± 1.5*inter-quartile distance

(IQR)), and the mean is displayed as + in **a**. All experiments except spatial distribution experiments for egl-30(ad805) (two repeats) were done in three repeats. Velocities of C. elegans N2, dgk-1(sy428), and eat-16(sa609) were compared (FR versus Control) using the Mann-Whitney testand velocity of egl-30 mutants were compared using the unpaired t-test. The spatial distribution of nematodes in the lawn was compared using the modified two sample binomial test (Wong et al., 2014) and the empirical standard deviation was presented as error bars. P > 0.05 = ns, P < 0.05 = *, P < 0.01 = **, P < 0.001 = ***, P < 0.0001 = ****

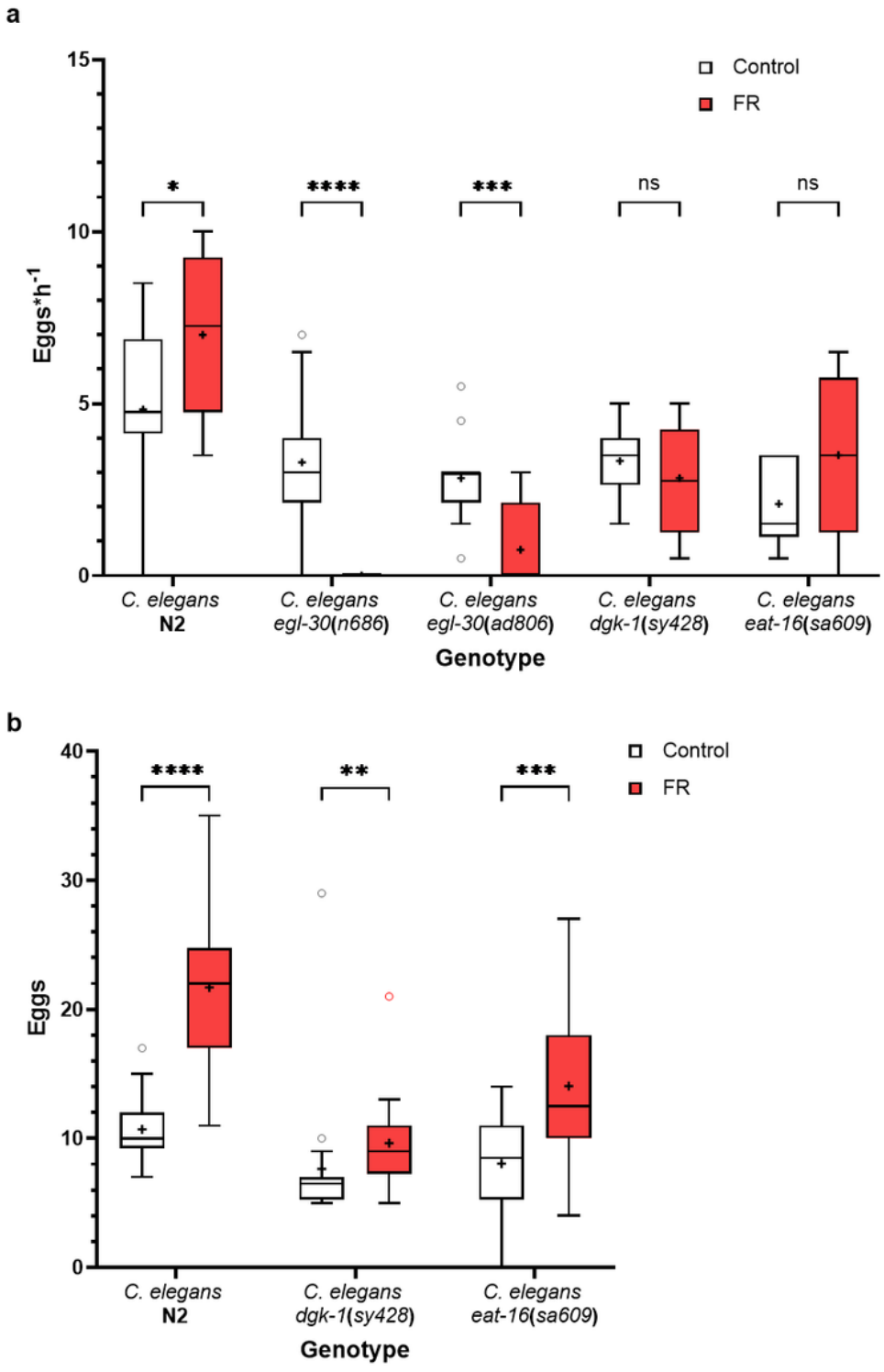

Figure 7

FR inhibits egg-laying of C. elegans. **a**Egg-laying rate for different C. elegans strains (Wildtype/N2, egl-30(n686), egl-30(ad806), dgk-1(sy428), and eat-16(sa609)) in presence (FR) or absence of FR (control). Both groups were grown until egg-laying adult stage on NGM plates covered with E. coli OP50 as food source mixed with 1 % DMSO, and FR for the FR group. 12 nematodes per group were analyzed individually for their egg-laying (Worms on FR were analyzed in presence of FR and similar for control). **b** Retained egg assay was performed with C. elegans N2, dgk-1(sy428), and eat-16(sa609)). Both groups were grown until egg-laying adult stage on NGM plates covered with E. coli OP50 as food source and 1% DMSO. For the FR group 2.5 mM FR were added to the food source. 20 nematodes per group were bleached and eggs were counted. Both **a** and **b** are presented as box and Tukey whiskers (Quartile ± 1.5*inter-quartile distance (IQR)) plot. The significance was evaluated using uncorrected multiple t-tests for **a**and C. elegans N2 and eat-16(sa609) in **b**, while dgk-1(sy428) in **b**was evaluated using Mann-Whitney test. P > 0.05 = ns, P < 0.05 = *, P < 0.01 = **, P < 0.001 = ***, P < 0.0001 = ****

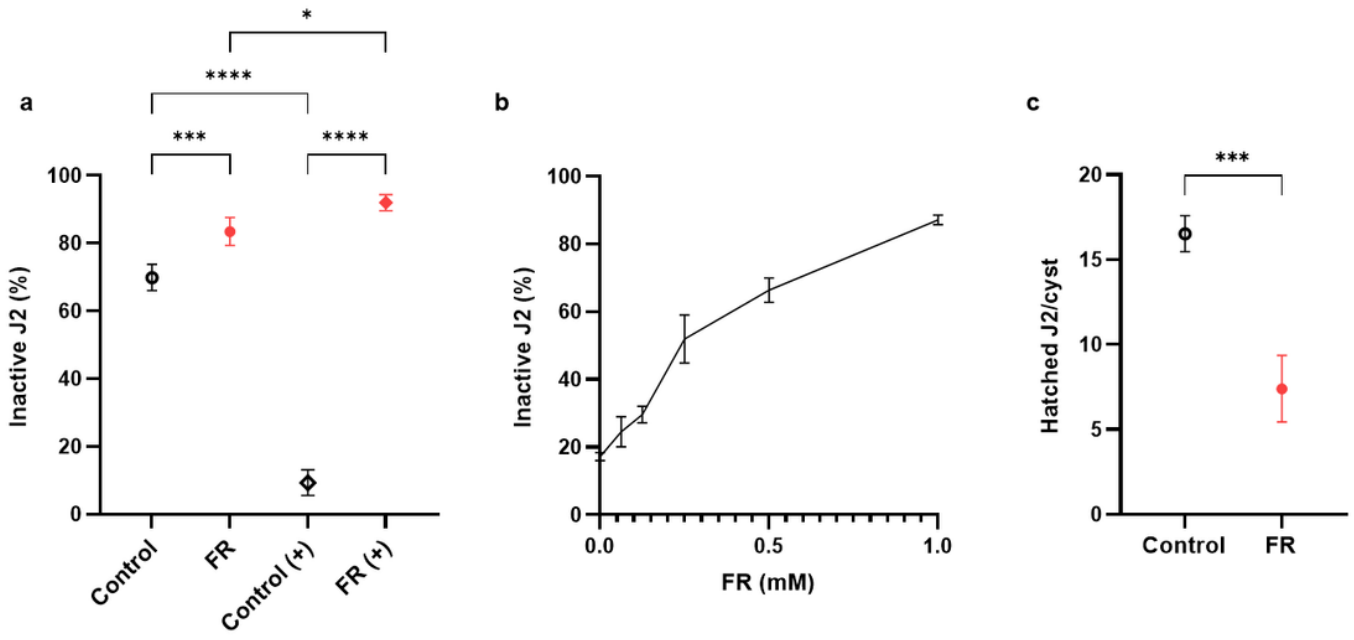

Figure 8

Effect of FR on movement **a**, **b** and hatching **c** of H. schachtii J2. **a** After incubation of H. schachtii J2 for 4 days in the presence of FR (1 mM) mixed with 1% DMSO (FR) or 1% DMSO (control) either with (+) or without octopamine the number of inactive (not bend or moving) and active worms was counted. The relative amount is depicted on the y-axis. The significance was evaluated using ordinary One-way ANOVA with Tukey's multiple comparisons test. **b**After incubation of H. schachtii J2 for 4 days in presence of six different FR concentrations (0, 0.0625, 0.125, 0.25, 0.5, 1 mM) mixed with 1% DMSO the number of inactive (not bend or moving) and active worms was counted. The relative amount is depicted on the y-axis. **c** Comparison of hatched H. schachtii juveniles per cyst with 1 mM FR disolved in 1% DMSO (FR) or

1% DMSO (control) after incubation of 7 days. The significance was evaluated using unpaired t-test. All experiments, n = 4. P > 0.05 = ns, P < 0.05 = *, P < 0.01 = **, P < 0.001 = ***, P < 0.0001 = ****

Supplementary Files

This is a list of supplementary files associated with this preprint. Click to download.

- supportinginformation1KoenigetalJOCE.docx
- supportinginformation2KoenigetalJOCE.xlsx